HOW DOES ANISOTROPIC FOCAL REGION CHANGE THE STRUCTURE OF THE MOMENT TENSOR ?

by

Dilay Poyraz

B.S., Geophysical Engineering, İstanbul University , 2016

Submitted to the Kandilli Observatory and Earthquake Research Institute in partial fulfillment of the requirements for the degree of Master of Science

Graduate Program in Geophysics

Boğaziçi University

2021

HOW DOES ANISOTROPIC FOCAL REGION CHANGE THE STRUCTURE OF THE MOMENT TENSOR ?

DATE OF APPROVAL: 19.02.2021

Dedicated to my beloved family.

ACKNOWLEDGEMENTS

First of all, I would like to thank my thesis advisor Dr.Çağrı Diner of the Geophysics Department at Boğaziçi University. His guidance helped me all the time in writing process of this thesis.

Especially, I would also like to thank Assoc. Prof. Dr.Ali Özgün Konca of the Geophysics Department at Boğaziçi University as the second reader of this thesis. He gave me all support whenever I needed it throughout the entire process. He always encouraged me and made me feel like I was part of this family.

I would like to thank Sezim Güvercin, Esra Ertan, Işınsu Çeker, Gökçe Öter, Deniz Ertuncay, all my professors and my classmates for their technical help and insightful comments.

Finally, I would like to thank my beloved family. They have always been with me and encouraged me all the time. They did not spare their material and spiritual support from me. This thesis would not have been finished without their supports, love them so much. Thank you.

ABSTRACT

HOW DOES ANISOTROPIC FOCAL REGION CHANGE THE STRUCTURE OF THE MOMENT TENSOR ?

In this study, we show how the invariants of the moment tensors change for different orientations of sources in a vertical transversely isotropic (TI) focal region. The invariants of the moment tensors, namely their norms, traces and eigenvalues, have physical interpretations such as seismic moment, isotropic-component and radiation pattern, respectively. Hence it is important to know how these values change for a given elasticity tensor of the focal region. These invariants strongly depend on the strength of anisotropy which is related with the variation of the eigenvalues of TI elasticity tensor from its closest-isotropic elasticity tensor.

We plotted the values of the projection for each 10-gridded orientations of slip and normal vectors around the unit sphere in order to see the distribution properly. Thus, we plotted the projection of source tensor **d** onto different eigenspaces. In doing so, various materials were used for data of elastic parameters and eigenvalues such as shale, dry-cracks etc. Then the norms of the elasticity tensors of various materials has been calculated and plotted. The maximum and minimum points in the norm plots and the ratios of the maximum and minimum eigenvalues of various materials were found to be similar to each other. The eigenvalues of moment tensor for different anisotropic focal regions have been shown. Thus, the relation between isotropic component amount and γ values were illustrated. Lastly, the strength of anisotropy is evaluated and related with the invariants of the moment tensors.

ÖZET

ANİZOTROPİK ODAK BOLGESİ MOMENT TENSORÜN YAPISINI NASIL DEĞİŞTİRİR ?

Bu çalışmada, dikey transvers izotropik (TI) odak bölgesindeki kaynakların farklı oryantasyonlar için moment tensörlerindeki değişmezlerin nasıl değiştiğini gösteriyoruz. Moment tensörlerinin değişmezleri, yani normları , izleri ve özdeğerleri, sırasıyla sismik moment, izotropik bileşen ve yayınım paterni gibi fiziksel yorumlara sahiptir. Bu sebeple, bu değerlerin odak bölgesinin belirli bir elastisite tensörü için nasıl değiştiğini bilmek çok önemlidir. Bu değişmezler, TI elastisite tensörünün özdeğerlerinin en yakın izotropik tensöründen değişimi ile ilişkili olan anizotropinin gücüne önemli bir şekilde bağlıdır.

Dağılımı düzgün görebilmek için küre etrafındaki her 10 gridli kayma yönü ve normal vektörler için izdüşüm değerlerini çizdik. Böylece, kaynak tensör d'nin farklı özuzaylara projeksiyonunu çizmiş olduk.Bunun için elastik parametreleri ve özdeğerleri verilen şeyl,kuru-çatlak gibi çeşitli materyaller kullanıldı.Daha sonra bu farklı malzemelerin normları hesaplanmış ve grafiğe dökülmüştür.Norm plotlarındaki maksimum ve minimum noktaları ile çeşitli materyallerin maksimum ve minimum özdeğerlerinin oranları alınarak birbirlerine ne kadar benzedikleri bulundu. Son olarak, anizotropinin gücü değerlendirilir ve moment tensörlerin değişmeyenleri ile ilişkilendirilir.

TABLE OF CONTENTS

LIST OF FIGURES

LIST OF TABLES

LIST OF SYMBOLS/ABBREVIATIONS

C_{ij}	2^{nd} order elasticity tensor
c_{ijkl}	4^{th} order elasticity tensor
D	Slip of a Fault (cm)
d	Fault Vector
e_i	Unit vector of i^{th} axis
$e_i^{'}$	Representation of an unit vector of i^{th} axis on a new coordinate frame
G_{np}	Green's Function
I	Identity Matrix
M	Moment Tensor
M_0	Seismic Moment
m	Moment Density Function
$\overline{m_1}$	Deviatoric Part of **M**
r	Distance of the Observation Point
S	Fault Area (km^2)
tr(M)	Trace of a matrix M
u	Slip Vector
u_n	Displacement on the n direction
v	Fault Normal
x	Location of Reciever
δ	Dip Angle of a Fault Plane
ϵ	Strain Tensor
θ	2^{nd} Euler Rotation Angle
λ	Rake Angle of a Fault Plane
μ	Rigidity
ξ_q	Location of a Source
Σ	Surface Area
σ	Stress Tensor
τ	Source Time

Φ	Strike Angle of a Fault Plane

LIST OF ABBREVIATIONS

CLVD	Compensated Linear Vector Dipole
DC	Double Couple
ISO	Isotropic
non-DC	non double couple
TI	Transversely Isotropic

1. INTRODUCTION

In Earth crust and upper mantle, anisotropy might be the extensive feature for geological structures [2, 20, 23].

Many geological developments may lead to anisotropy such as sedimentary layering, fractures or cracks. It is a well-known fact that seismic observations are affected by anisotropy significantly. For instance, when seismic source is located inside an anisotropic medium, the waves generated are affected and leads to different radiation patterns. So the seismic wave propagations are affected by anisotropy eventually [29]. Therefore many scientists have studied anisotropy in order to understand how anisotropy affects the seismic waves and their wave propagation [2, 9, 12, 18, 29].

After that the scientist had curiosity about that the generation of seismic waves are affected by which anisotropy type in order to estimate the anisotropy type. But too many problems must have to solved. One of them is Greens function calculation [3, 4, 5, 7, 9, 11, 19, 26]. And the second one is calculating the seismic moment tensor in anisotropic focal media and its focal mechanisms. Kawasaki & Tanimato [15] have illustrated that in anisotropic focal media shear faulting might produce the mechanisms with non- DC components. Many scientist have been also mentioned and discussed the anisotropy as a possible cause of non-DC mechanisms [10, 13, 14, 21, 27, 28, 29].

Understanding the structure of the moment tensor plays a significant role to define seismic sources effectively. Studies of the full moment tensor inversions shows that some events have non-DC moment tensor structure. In other words these kind of events have both isotropic (ISO) and compensated linear vector dipole(CLVD) such as volcanic activities, nuclear explosions, hydraulic fracturing.

The goal of this thesis is to show how the invariants of the moment tensors change for different orientations of sources in a vertical transversely isotropic (TI) focal region. It is important to know how these values change for a given elasticity tensor of the focal region.

In Chapter 2, equation of motion and its green's function solution are shown. The relation between the definition of moment density tensor and point source assumption is stated. Moment and source tensors are expressed in Kelvin notation and moment tensor decomposition is shown. In Chapter 3, eigenspaces of TI elasticity tensors and isotropic(ISO) elasticity tensors are shown. In Chapter 3, for each 10-gridded orientations of the slip and normal vectors around the unit sphere, the values of the projections, namely $(\Sigma^i.\mathbf{d})$, are plotted on the steographic projection net for different materials. Norm of a moment tensor is expressed and plotted for different materials. Distribution of the isotropic percentage of the moment tensor which has different source orientations is shown. In order to understand the mechanism of seismic source, the eigenvalues of the moment tensor is used. The eigenvalues of moment tensors of seismic sources occurring in different anisotropic focal regions are plotted on the basic lune. Lastly, the deviation angles of the eigenvectors for different source orientations is plotted.

2. THEORETICAL BACKGROUND

2.1. Equation of Motion

Equation of motion can be written by using Newton's second law as

$$\rho(x)\ddot{U}_i = f_i(\mathbf{x},t) + \sigma_{ij,j} \ , \qquad i \in \{1,2,3\} \tag{2.1}$$

where density ρ, dots over a symbol imply time derivative, displacement is U, body force is f_i, $\mathbf{x}$ is spatial variable and t is time, σ_{ij} denotes stress tensor. Comma after indices indicates spatial derivative. Throughout this text, Einstein's summation convention will be used, i.e. repeated indices imply summation.

The stress and strain of the material are connected by a linear relationship which is called Hooke's law.

$$\sigma_{ij} = C_{ijkl}\varepsilon_{kl}, \tag{2.2}$$

where C_{ijkl} is a fourth rank tensor which represents elastic parameters of medium. The strain tensor, denoted by ε_{kl}, can be defined in terms of displacements as

$$\varepsilon_{kl} = \frac{1}{2}(U_{k,l} + U_{l,k}). \tag{2.3}$$

Substituting the definition of strain tensor into Hooke's law, stress tensor can be obtained as

$$\begin{aligned}
\sigma_{ij} &= C_{ijkl}\frac{1}{2}(U_{k,l}+U_{l,k}) \\
&= \frac{1}{2}(C_{ijkl}U_{k,l}+C_{ijkl}U_{l,k}) \\
&= \frac{1}{2}(C_{ijkl}U_{k,l}+C_{ijkl}U_{l,k}) \quad \text{since } C_{ijkl}=C_{ijlk} \\
&= C_{ijkl}U_{k,l} \quad \text{because of Einstein's summation convention.} \qquad (2.4)
\end{aligned}$$

Note that $C_{ijkl}=C_{ijlk}$ due to the symmetry of elasticity tensor.

If equation (2.2) is applied to equation (2.1), the equation of motion becomes vector wave equation in the absence of interior body force

$$\begin{aligned}
\rho\ddot{U}_i &= C_{ijkl}U_{k,lj} \\
&= (C_{ijkl}U_{kl})_{,j} \\
&= C_{ijkl,j}U_{k,l}+C_{ijkl}U_{k,lj} \\
&= C_{ijkl}U_{k,lj}, \qquad (2.5)
\end{aligned}$$

assuming that the medium is homogeneous i.e. $C_{ijkl,j}=0$. Equation (2.5) is the vector wave equation in homogeneous, anisotropic medium.

2.2. Green's Function Solution of Vector Wave Equation

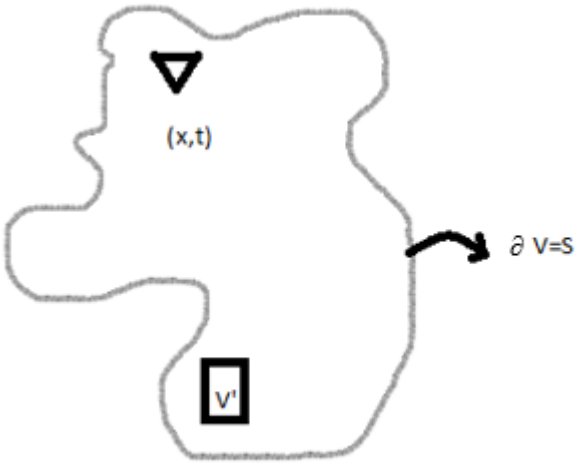

Figure 2.1. Representation of domain (V), measurement points ((x,t)), boundary (δV), and the source region ($V\prime$).

Assume that we want to solve vector wave equation (2.4) in medium V in order to have a unique solution **U** of equation (2.4), boundary conditions of U should be given.

Green's function can be defined as the response of the medium to unique impulse. Unit impulse means a signal whose momentum is equal to unity. More Precisely unit impulse is defined by Dirac delta function.

Definition of Dirac Delta Function

$\delta(x - x_0)\delta(t - t_0) = 0$, $\forall x \neq x_0$ and $t \neq t_0$ and

$$\iiint_V \delta(x - x_0)\delta(t - t_0)\, dx\, dt = 1 \tag{2.6}$$

Suppose that for unit impulse ($\delta(x-x_0)(t-t_0)$),response function is known which is $G(x,t;x_0,t_0)$. In other words Green's function satisfy the following equation

$$C_{ijkl}G_{k,lj} - \rho\ddot{G}_i = \delta(t-t_0)\delta(x-x_0). \tag{2.7}$$

Then the solution for the displacement can be given as

$$\begin{aligned} U_n(x,t) = &\iiint_V f(x',t')G_{ni}(x,t;x',t')\,dv(x') \\ &+ \iint_\Sigma h_i(x,t)G_{n,k}(x,t;x',t')\,d\Sigma, \end{aligned} \tag{2.8}$$

where $U_n(x,t)$ is n-th component of the displacement at the receiver location and time, $G_{ni}(x,t;x',t')$ is the n-th component of the displacement at (x,t) due to the source along i-th direction at (x',t'),((x,t)) is receiver location and time, ((x',t')) is source location and time.$h_i(x,t)$ is traction boundary condition. The solution 2.10 can be modified for faulting problems as

$$U_n(x,t) = \iint_\Sigma [U_i(\xi,\tau)]\hat{n}_j(\xi)C_{ijkl} * G_{nk,l}(x,t;\xi,\tau)\,d\Sigma(\xi) \tag{2.9}$$

where $U_n(x,t)$ is displacement at the receiver, $[U_i(\xi,\tau)]$ is slip which means displacement at the fault, $\hat{n}_j(\xi)$ is unit normal vector of the fault, $C_{ijkl}(\xi)$ is elasticity tensor of the source region, (x,t) is receiver point and time, (ξ,τ) is a fault point and time and $G_{nk,l}(x,t;\xi,\tau)$is Green's function of the medium which means response of the Dirac-delta at the point ξ and τ.

2.3. Definition of Moment Density Tensor versus Point Source Assumption

Observe that $U_i(\xi,\tau)\hat{n}_j(\xi)C_{ijkl}$ represents the fault source in equation 2.9.

The solution $[U_n](x,t)$ can also be written as,

$$U_n(x,t) = \iint_\Sigma M_{kl}(\xi,\tau) * G_{nk,l}(x,t;\xi,\tau)\,d\Sigma \tag{2.10}$$

$$M_{kl} = [U_i(\xi,\tau)]\hat{n}_j C_{ijkl} \tag{2.11}$$

where $M_{kl}(\xi,\tau)$ is called the moment density tensor.In order to avoid taking integral in the expression of $U_n(x,t)$, assuming that;
i)n is constant throughout the surface Σ which is a plane,
ii)C_{ijkl} is a constant on the plane Σ and the focal region is assumed to be isotropic. In general, seismologists are more prone to use point source by choosing the periods of data for surface Σ. Point source assumption is the waves which are radiated from the different elements $d\Sigma$ are approximately in phase [1]. Therefore, the displacement field at the receiver point is found by convolving the moment density tensor at the different points of the fault with the Green's function. When ξ is fixed, then expression is given in equation (2.9) can be written as

$$\begin{aligned} M_{kl} &= \iint_{\Sigma} [U_i(\xi,\tau)]\hat{n}_j(\xi) C_{ijkl}(\xi) * G_{nk,l}(x,t;\bar{\xi},\tau)\, d\Sigma, \\ &= \Big(\iint_{\Sigma} [U_i(\xi,\tau)]\hat{n}_j(\xi) C_{ijkl}(\xi)\, d\Sigma\Big) * G_{nk,l}(x,t;\bar{\xi},\tau) \end{aligned} \tag{2.12}$$

where $\bar{\xi}$ might be taken as the centroid of the earthquake, thus, Green's function can be taken out from integral.Thus, the point source moment density tensor can be written as

$$M_{kl} = \iint_{\Sigma} [U_i(\xi,\tau)]\hat{n}_j(\xi) C_{ijkl}(\xi)\, d\Sigma. \tag{2.13}$$

Suppose that Σ is a planar surface, $\hat{n}$ can be taken out from the integral due to the fact that $\hat{n}$ does not change according to different surface elements.Furthermore, C_{ijkl} can be taken as a constant on the fault plane, so, the moment density tensor expressed in equation (2.12) becomes

$$M_{kl} = \hat{n}_j C_{ijkl} \iint_{\Sigma} [U_i]\, d\Sigma, \tag{2.14}$$

To consider the slip as a constant, slip at the fault must be divided by the area of the fault surface which is $A = \iint_{\Sigma} d\Sigma$. Then the moment tensor of a point source can be shown as

$$M_{kl} = [\bar{U}_i] n_j C_{ijkl}, \tag{2.15}$$

whereM_{kl} is thepoint source moment tensor and $n = A\hat{n}_j$is the fault normal vector whose magnitude is the area of the fault plane. $[\bar{U}]$ is constant.

Thus, the displacement at the receiver point and time (x,t)can be evaluated as

$$U_n(x,t) = M_{kl} * G_{nk,l}(x,t;\bar{\xi},\tau). \tag{2.16}$$

where M_{kl} is the point source moment tensor explained in equation(2.15).

The difference between the moment density tensor and moment tensor is that the moment tensor of point source which expressed in equation(2.15) has a fault normal whose magnitude is equal to the fault area, however the moment density tensor includes a unit fault normal vector.

2.4. Moment and Source Tensor Expressed in Kelvin Notation

The purpose of this section is in order to show that the point-source moment tensor can be written as matrix equation. In other words, we want to write down moment tensor as a vector and elasticity tensor as a matrix. By doing this, linear algebra operations can be easily applied [6].

In order to do so, equation (2.15) can be written by using the source tensor instead of **u** and **n**. Then the moment tensor expression becomes

$$\begin{aligned} M_{kl} &= \frac{1}{2} C_{ijkl}([U_i(\xi,\tau)]n_j + [U_j(\xi,\tau)]n_i) \\ &= C_{ijkl} D_{ij}, \end{aligned} \tag{2.17}$$

where in order to simplify the notation, the average and constant slip function have been denoted by $[U_i]$ instead of $[\bar{U}_i]$. The first equality follows from the symmetry of the elasticity tensor i.e. $C_{ijkl} = C_{jikl}$.For second equality, the second-rank tensor $D_{ij}$is defined by the tensor product of $[\mathbf{U}]$ and $\mathbf{n}$ as

$$D_{ij} = \frac{1}{2}([U_i]n_j + [U_j]n_i), \tag{2.18}$$

$$= \frac{1}{2}\begin{bmatrix} 2[U_1]n_1 & [U_1]n_1 + [U_2]n_1 & [U_1]n_3 + [U_3]n_1 \\ [U_1]n_1 + [U_2]n_1 & 2[U_2]n_2 & [U_2]n_3 + [U_3]n_2 \\ [U_1]n_3 + [U_3]n_1 & [U_2]n_3 + [U_3]n_2 & 2[U_3]n_3 \end{bmatrix} \tag{2.19}$$

where $\mathbf{D}$ is known as the source tensor or potency tensor (Vavrycuk,2005). Equation (2.18) can be written using tensor product as

$$D = \frac{1}{2}([\mathbf{U}] \otimes \mathbf{n} + \mathbf{n} \otimes [\mathbf{U}]), \tag{2.20}$$

where the components of the tensor product is indicated as $\mathbf{a} \otimes \mathbf{b} = a_i b_j$.

Note that equation (2.17) has the same form of Hooke's law, in other words the fourth-rank tensor relates two second rank tensor. Hence, it can be written in a matrix form using Kelvin notation.The biggest advantage of Kelvin notation is that using theorems and tools of linear algebra such as determining its eigenvalues, eigenvectors and decomposing the elasticity tensor. For using Kelvin representation, norm preserving map should be defined from the space of symmetric second-rank tensors to six-dimensional vectors such as

$$\begin{bmatrix} M_{11} & M_{12} & M_{13} \\ M_{12} & M_{22} & M_{23} \\ M_{13} & M_{32} & M_{33} \end{bmatrix} \rightarrow \begin{bmatrix} M_{11} \\ M_{22} \\ M_{33} \\ \sqrt{2}M_{23} \\ \sqrt{2}M_{13} \\ \sqrt{2}M_{12} \end{bmatrix}, \begin{bmatrix} D_{11} & D_{12} & D_{13} \\ D_{12} & D_{22} & D_{23} \\ D_{13} & D_{32} & D_{33} \end{bmatrix} \rightarrow \begin{bmatrix} D_{11} \\ D_{22} \\ D_{33} \\ \sqrt{2}D_{23} \\ \sqrt{2}D_{13} \\ \sqrt{2}D_{12} \end{bmatrix} \tag{2.21}$$

Since this moment tensor is symmetrical, it is sufficient to use only 6 parameters when writing in vector notation as shown in equation (2.21). Likewise,the elasticity tensor can be represented by 6x6 matrix as [6].

$$C = \begin{bmatrix} C_{1111} & C_{1122} & C_{1133} & \sqrt{2}C_{1123} & \sqrt{2}C_{1113} & \sqrt{2}C_{1112} \\ C_{1122} & C_{2222} & C_{2233} & \sqrt{2}C_{2223} & \sqrt{2}C_{2213} & \sqrt{2}C_{2212} \\ C_{1133} & C_{1133} & C_{3333} & \sqrt{2}C_{3323} & \sqrt{2}C_{3313} & \sqrt{2}C_{3312} \\ \sqrt{2}C_{1123} & \sqrt{2}C_{2223} & \sqrt{2}C_{3323} & 2C_{2323} & 2C_{2313} & 2C_{2312} \\ \sqrt{2}C_{1113} & \sqrt{2}C_{2213} & \sqrt{2}C_{3313} & 2C_{2313} & 2C_{1313} & 2C_{1312} \\ \sqrt{2}C_{1112} & \sqrt{2}C_{2212} & \sqrt{2}C_{3312} & 2C_{2312} & 2C_{1312} & 2C_{1212} \end{bmatrix} \tag{2.22}$$

Note that the inputs in the right-top corner of the matrix appears two times in the elasticity tensor, for example, $C_{1123} = C_{1132}$. Likewise, the items in the down right corner appears four times such as $C_{2313} = C_{2331} = C_{3213} = C_{3231}$. On the other hand, the items in the left-top corner appears only once. Hence, the coefficient $\sqrt{2}, 2, 1$ appears in the matrix representation respectively.

The equation (2.17) can be written by using matrix representation as

$$m = Cd, \qquad \text{or} \tag{2.23}$$

$$\begin{bmatrix} m_1 \\ m_2 \\ m_3 \\ \sqrt{2}m_4 \\ \sqrt{2}m_5 \\ \sqrt{2}m_6 \end{bmatrix} = \begin{bmatrix} C_{11} & C_{12} & C_{13} & \sqrt{2}C_{14} & \sqrt{2}C_{15} & \sqrt{2}C_{16} \\ C_{12} & C_{22} & C_{23} & \sqrt{2}C_{24} & \sqrt{2}C_{25} & \sqrt{2}C_{26} \\ C_{13} & C_{23} & C_{33} & \sqrt{2}C_{34} & \sqrt{2}C_{35} & \sqrt{2}C_{36} \\ \sqrt{2}C_{14} & \sqrt{2}C_{24} & \sqrt{2}C_{34} & 2C_{44} & 2C_{45} & 2C_{46} \\ \sqrt{2}C_{15} & \sqrt{2}C_{25} & \sqrt{2}C_{35} & 2C_{45} & 2C_{55} & 2C_{56} \\ \sqrt{2}C_{16} & \sqrt{2}C_{26} & \sqrt{2}C_{36} & 2C_{46} & 2C_{56} & 2C_{66} \end{bmatrix} \begin{bmatrix} d_1 \\ d_2 \\ d_3 \\ \sqrt{2}d_4 \\ \sqrt{2}d_5 \\ \sqrt{2}d_6 \end{bmatrix} \tag{2.24}$$

Square root of two in this equation only appear in off-diagonals because they are set to be equal in norms.

The following replacements indicate the indices of the tensors
$(1,1) \rightarrow 1$, $(2,2) \rightarrow 2$,$(3,3) \rightarrow 3$,
$(2,3) \rightarrow 4$,$(1,3) \rightarrow 5$,$(1,2) \rightarrow 6$.

Kelvin notation preserves the norms of the corresponding structures, thus, the elasticity matrix can be declared as a linear transformation in $\mathbb{R}^6$ now by using the advantages of linear algebra.

2.5. Decomposition of the Moment Tensor

Equivalent body forces at a seismic point source can be identified as the moment tensor [8]. Moment tensors are used from small discharges to great earthquakes. Double-couple (DC) type of the moment tensor denotes the equivalent of forces of shear faulting acting on a planar fault in isotropic media. On the other hand, a lot of studies have evaluated that seismic sources might show non-double-couple (non-DC) components of the moment tensors [13, 17].

For instance an explosion might be the good example for non-DC source. But non-DC can also be generated by collapse of a mine caves in a shear faulting with non-planar fault [22, 24].

Moment tensor decomposition was proposed by Knopoff & Randall [16] in 1970 in order to detect which type of moment tensor should be used. They have divided the moment tensor into three fundamental parts which are isotropic (ISO), Compensated Linear Vector Dipole (CLVD), and Double-Couple (DC). There are many moment tensor decompositions. But this one is broadly accepted due to this proposal was proved to be useful for many physical interpretations and many scientist have studied on this decomposition and further developed it. We need efficient moment tensor decomposition in order to interpret the source elaborative.

In order to decompose a moment tensor, firstly, moment tensor M is diagonalized and reconstituded to three types of source such as ISO, DC, CLVD.

Moment tensor decomposition can be shown as,

$$\mathbf{M} = \mathbf{M}^{ISO} + \mathbf{M}^{DC} + \mathbf{M}^{CLVD}, \tag{2.25}$$

For decomposing the seismic moment tensor, eigenvalues and orthonormal basis of eigenvectors are used.

$$\mathbf{M} = \mathbf{M}_1 e_1 \otimes e_1 + \mathbf{M}_2 e_2 \otimes e_2 + \mathbf{M}_3 e_3 \otimes e_3 \tag{2.26}$$

where

$$\mathbf{M}_1 \geq \mathbf{M}_2 \geq \mathbf{M}_3 \tag{2.27}$$

e_1, e_2 and e_3 are vectors that they can be expressed as T (tension), N (null) and P (pressure) axes respectively. The symbol "$\otimes$" illustrates cross-product of two vectors.

There are two elementary properties of moment tensor and these are separated in Equation (2.26) : One of them is the orientation of source and the other one is type and size of the fault. All of those properties are defined by three eigenvectors and eigenvalues of $\mathbf{M}$ respectively. Considering physical reasons, the three reasons in Equation (2.26) can be reconstructed as Isotropic (ISO), Double-Couple (DC) and Compensated Linear Vector Dipole (CLVD) parts Figure (2.2) as [16].

$$\begin{aligned} \mathbf{M} &= \mathbf{M}_{ISO} + \mathbf{M}_{DC} + \mathbf{M}_{CLVD} \\ &= \mathbf{M}_{ISO}\mathbf{E}_{ISO} + \mathbf{M}_{DC}\mathbf{E}_{DC} + \mathbf{M}_{CLVD}\mathbf{E}_{CLVD} \end{aligned} \tag{2.28}$$

where $\mathbf{E}_{ISO}, \mathbf{E}_{DC}, \mathbf{E}_{CLVD}$ are the elementary tensors of the ISO, DC and CLVD. $\mathbf{M}_{ISO}, \mathbf{M}_{DC}, \mathbf{M}_{CLVD}$ are the moments of ISO, DC and CLVD.

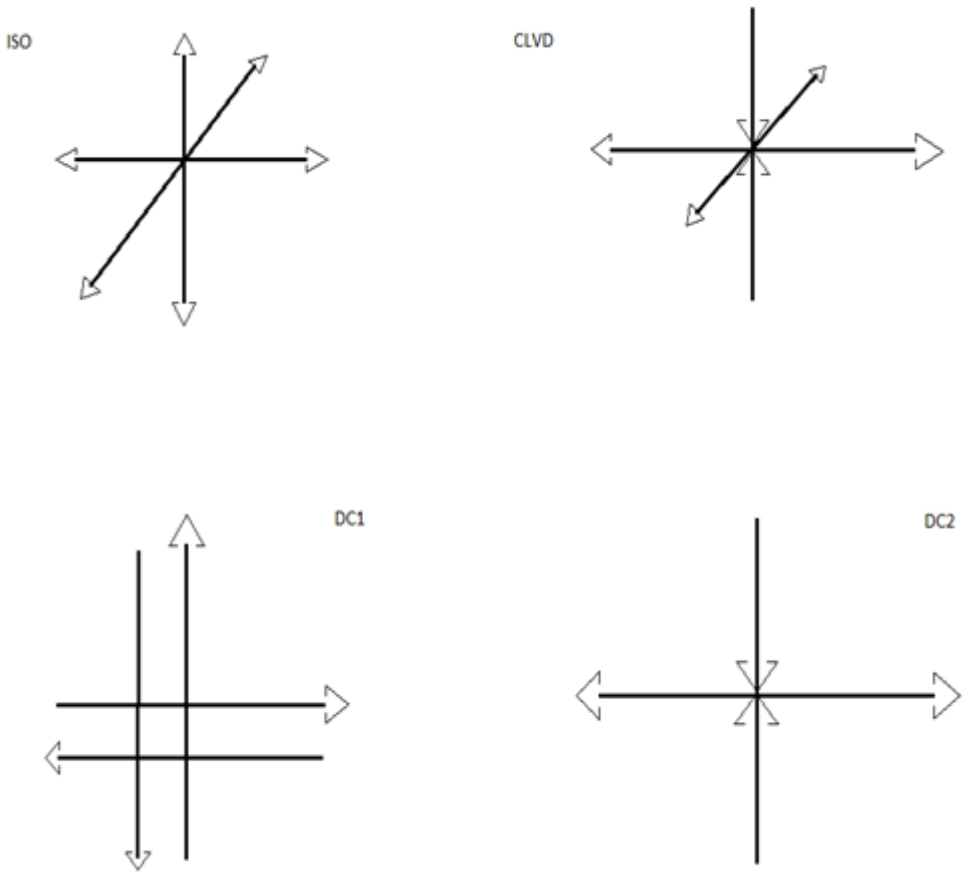

Figure 2.2. Reconstruction of ISO, DC and CLVD parts of moment tensor.

The base tensors can be shown as [31];

$$\mathbf{E}_{ISO} = \begin{bmatrix} 1 & 0 & 0 \\ 0 & 1 & 0 \\ 0 & 0 & 1 \end{bmatrix}, \mathbf{E}_{DC} = \begin{bmatrix} 1 & 0 & 0 \\ 0 & 0 & 0 \\ 0 & 0 & -1 \end{bmatrix},$$

$$\mathbf{E}^{+}_{CLVD} = \frac{1}{2}\begin{bmatrix} 2 & 0 & 0 \\ 0 & -1 & 0 \\ 0 & 0 & -1 \end{bmatrix}, \mathbf{E}^{-}_{CLVD} = \frac{1}{2}\begin{bmatrix} 1 & 0 & 0 \\ 0 & 1 & 0 \\ 0 & 0 & -2 \end{bmatrix}, \tag{2.29}$$

$\mathbf{E}_{CLVD}$ is consist of $\mathbf{E}^{-}_{CLVD}$ and $\mathbf{E}^{+}_{CLVD}$. $\mathbf{E}^{+}_{CLVD}$ is used if $M_1 + M_3 - 2M_2 \geq 0$, likewise $\mathbf{E}^{-}_{CLVD}$ is used if$M_1 + M_3 - 2M_2 < 0$. Consequently, CLVD tensor is aligned the axis with the deviatoric eigenvalue whic has the largest magnitude. The Unit Spectral Norm is maximum dipole force of the base tensor is unity (Figure 2.2).

The values M_{ISO},M_{CLVD} and M_{DC} which are defined in (2.28) can be shown as follows

$$M_{ISO} = \frac{1}{3}(M_1 + M_2 + M_3), \tag{2.30}$$

$$M_{CLVD} = \frac{2}{3}(M_1 + M_3 - 2M_2), \tag{2.31}$$

$$M_{DC} = \frac{1}{2}(M_1 - M_3 - |M_1 + M_3 - 2M_2|), \tag{2.32}$$

where M_{CLVD} comprises the sign of the elementary CLVD tensor. MCLVD is calculated as the value of equation (2.31) when the elementary CLVD tensor (E_{CLVD}) is considered with its sign as in Equation (2.28).

In Equations (2.30,2.31,2.32) which are expressed above the values M_{ISO},M_{CLVD} and M_{DC} are normalized and denoted with seismic moment M. Moreover,the scale factors of M_{ISO},M_{CLVD} and M_{DC} are C_{ISO},C_{CLVD} and C_{DC} respectively. In order to determine;

$$\begin{bmatrix} C_{ISO} \\ C_{CLVD} \\ C_{DC} \end{bmatrix} = \frac{1}{M} \begin{bmatrix} M_{ISO} \\ M_{CLVD} \\ M_{DC} \end{bmatrix} \tag{2.33}$$

To clear M up ;

$$M = |M_{ISO}| + |M_{CLVD}| + M_{DC} \tag{2.34}$$

Following equation is fulfilled by the scales factors C_{ISO},C_{CLVD} and C_{Dc}.

$$1 = |C_{ISO}| + |C_{CLVD}| + C_{DC} \tag{2.35}$$

C_{DC} is always positive which is implied by Equations (2.30,2.31,2.32,2.33,2.34) and in range from 0 to 1. C_{CLVD} and C_{ISO} are in range from -1 to 1.

As a result the decomposition of moment tensor M is showed below.

$$\mathbf{M} = M(C_{ISO}\mathbf{E}_{ISO} + C_{DC}\mathbf{E}_{DC} + |C_{CLVD}|\mathbf{E}_{CLVD}) \tag{2.36}$$

Where norm of $\mathbf{M}$ is M and calculated using Eqn (2.34). The absolute value of CLVD term is used due to the fact that the sign of the CLVD is included in elementary tensor $\mathbf{E}_{CLVD}$[30].

3. RESULTS

3.1. Shear Source In Anisotropic Focal Region

We know that Hooke's law is used for elastic cases. But once the fault has been ruptured, which means a permanent deformation, the behaviour of source is no longer elastic. Hence Hooke's law becomes inappropriate for faults. In other words, during rupture the stress is finite on the fault. In this case the generalized Hooke's law is used as

$$\mathbf{M} = \mathbf{CD}, \tag{3.1}$$

where M is moment tensor and C is elasticity tensor. M is proportional to D when the medium is isotropic. In other words M and D have same eigenvectors.

The moment tensor of shear source occurs in transversal isotropic(TI) focal region and depends on two angles
i) angle between the normal vector of fault and the infinite-fold rotation axis of TI elasticity tensor,
ii) angle between the slip and the symmetry plane of the TI elasticity tensor.

Depending on those angles the norm of the moment tensor and the eigenvalues of moment tensor change with respect to the symmetry axes of a TI elasticity tensor. After observing this fact, we define moment tensor as an image of shear source under the transformations in terms of TI elasticity tensor.

In order to consider the eigendecomposition of elasticity tensor C, it can be written in tensor notation as

$$\begin{aligned} C = {} & \lambda_1^C(\hat{\mathbf{\Sigma}}^{\mathbf{1}} \otimes \hat{\mathbf{\Sigma}}^{\mathbf{1}}) + \lambda_2^C(\hat{\mathbf{\Sigma}}^{\mathbf{2}} \otimes \hat{\mathbf{\Sigma}}^{\mathbf{2}}) + \lambda_3^C(\hat{\mathbf{\Sigma}}^{\mathbf{3}} \otimes \hat{\mathbf{\Sigma}}^{\mathbf{3}}) \\ & + \lambda_4^C(\hat{\mathbf{\Sigma}}^{\mathbf{4}} \otimes \hat{\mathbf{\Sigma}}^{\mathbf{4}}) + \lambda_5^C(\hat{\mathbf{\Sigma}}^{\mathbf{5}} \otimes \hat{\mathbf{\Sigma}}^{\mathbf{5}}) + \lambda_6^C(\hat{\mathbf{\Sigma}}^{\mathbf{6}} \otimes \hat{\mathbf{\Sigma}}^{\mathbf{6}}), \end{aligned} \tag{3.2}$$

where Σ's denotes that the six eigenvectors with the corresponding eigenvalues λ_i^C.

A TI elasticity tensor has four eigenspaces due to the fact that two of the eigenvalues duplicate two times. The eigenvectors of a TI elasticity tensor are shown in Table 3.2 when the layers of a subsurface are horizontal [6].

Table 3.1: The Eigenvalues and Eigenvectors of TI Elasticity Tensor.

Eigenvectors of TI Elasticity Tensor	TI Eigenvalues
$\Sigma^1 = (\frac{1}{\sqrt{2+\gamma^2}})(1, 1, \gamma, 0, 0, 0)$	λ_1^{TI}
$\Sigma^2 = (\frac{1}{\sqrt{4+2\gamma^2}})(\gamma, \gamma, -2, 0, 0, 0)$	λ_2^{TI}
$\Sigma^3 = (0, 0, 0, 1, 0, 0)$	λ_3^{TI}
$\Sigma^4 = (0, 0, 0, 0, 1, 0)$	$\lambda_4^{TI} = \lambda_3^{TI}$
$\Sigma^5 = (0, 0, 0, 0, 0, 1)$	λ_5^{TI}
$\Sigma^6 = (\frac{1}{\sqrt{2}})(1, -1, 0, 0, 0, 1)$	$\lambda_6^{TI} = \lambda_5^{TI}$

Herein $\gamma \in \mathbb{R}$ denotes the ratio of the strains along the z- axis with respect to any axis in the xy-plane for TI media.

In order to compare the eigenspaces of TI elasticity tensor and Isotropic elasticity tensor, eigenvectors and eigenvalues of Isotropic elasticity tensor are shown as

Table 3.2: The Eigenvalues and Eigenvectors of ISO(Isotropic) Elasticity Tensor.

Eigenvectors of ISO Elasticity Tensor	ISO Eigenvalues
$\Sigma^1 = (\frac{1}{\sqrt{3}})(1, 1, 1, 0, 0, 0)$	$\lambda_1^{iso} = 3\lambda + 2\mu$
$\Sigma^2 = (\frac{1}{\sqrt{6}})(1, 1, -2, 0, 0, 0)$	$\lambda_2^{iso} = 2\mu$
$\Sigma^3 = (0, 0, 0, 1, 0, 0)$	$\lambda_3^{iso} = 2\mu$
$\Sigma^4 = (0, 0, 0, 0, 1, 0)$	$\lambda_4^{iso} = 2\mu$
$\Sigma^5 = (0, 0, 0, 0, 0, 1)$	$\lambda_5^{iso} = 2\mu$
$\Sigma^6 = (\frac{1}{\sqrt{2}})(1, -1, 0, 0, 0, 1)$	$\lambda_6^{iso} = 2\mu$

where μ and λ are Lamé parameters.

The difference between the two tables is in ISO tensor, γ is taken as unity due to the fact that all directions are equivalent.

The word isotropic was used in two different ways. The first use, which were used former, means the isotropy class of the fourth-rank elasticity tensors. Then the second one is used for isotropic matrices. These isotropic matrices can be described as proportional to identity matrix.

In order to comprehend the relation between the eigenvalues of transversely isotropic (TI) elasticity tensors and their the closest-isotropic elasticity tensors, the following approximation can be used

$$\lambda_1^{iso} \approx \lambda_1^{TI} \tag{3.3}$$

$$\lambda_2^{iso} \approx \frac{\lambda_2^{TI} + 2\lambda_3^{TI} + 2\lambda_5^{TI}}{5} \tag{3.4}$$

where the expression of the second approach is that shear modulus is proportional to average TI eigenvalues which matches up with the deviatonic eigenspace. On the other hand if γ does not equal to 1, Σ^2 would not be a deviatoric tensor. Taking the orthogonal projection of TI tensor on to the elasticity tensor's isotropic linear subspace may be an expression of how the closest-isotropic tensor is found.

The form of the moment tensor occurring in TI focal region can be found by using equation (3.2) as

$$\begin{aligned} m &= Cd \\ &= \lambda_1^C(\hat{\mathbf{\Sigma}}^{\mathbf{1}}.\mathbf{d})\hat{\mathbf{\Sigma}}^{\mathbf{1}} + \lambda_2^C(\hat{\mathbf{\Sigma}}^{\mathbf{2}}.\mathbf{d})\hat{\mathbf{\Sigma}}^{\mathbf{2}} + \lambda_3^C(\hat{\mathbf{\Sigma}}^{\mathbf{3}}.\mathbf{d})\hat{\mathbf{\Sigma}}^{\mathbf{3}} \\ &\quad +\lambda_4^C(\hat{\mathbf{\Sigma}}^{\mathbf{4}}.\mathbf{d})\hat{\mathbf{\Sigma}}^{\mathbf{4}} + \lambda_5^C(\hat{\mathbf{\Sigma}}^{\mathbf{5}}.\mathbf{d})\hat{\mathbf{\Sigma}}^{\mathbf{5}} + \lambda_6^C(\hat{\mathbf{\Sigma}}^{\mathbf{6}}.\mathbf{d})\hat{\mathbf{\Sigma}}^{\mathbf{6}}. \end{aligned} \tag{3.5}$$

In Table (3.2) degenerated eigenspaces of TI elasticity tensors were shown, therefore Equation (3.5) can be written as follows

$$\mathbf{m} = \lambda_1^{TI}(\hat{\Sigma^1}.d)\hat{\Sigma^1} + \lambda_2^{TI}(\hat{\Sigma^2}.d)\hat{\Sigma^2} + \lambda_3^{TI}((\hat{\Sigma^3}.d)\hat{\Sigma^3} + (\hat{\Sigma^4}.d)\hat{\Sigma^4}) + \lambda_5^{TI}((\hat{\Sigma^5}.d)\hat{\Sigma^5} + (\hat{\Sigma^6}.d)\hat{\Sigma^6}) \tag{3.6}$$

It can be said that every moment tensor of a seismic source which occur in an anisotropic focal region is a linear combination of the eigenvectors of the elasticity tensor of that focal region. In other words, the coefficients can be expressed as the eigenvalues of the elasticity tensor and projection of d onto the eigenspaces. And these coefficients also determine the space of all moment tensors which are occured in an anisotropic focal region. Moreover, when the orientation of d change (strike,dip,rake), the structures of moment change e.g. their norms, eigenvalues, traces.

3.2. Projections of Source Tensors Onto The Eigenspaces of Elasticity Tensor

In anisotropic focal region, the structure of the moment tensor hinges on the coefficients of the bases vectors that are the eigenvectors of elasticity tensor. These values of projections may change for various orientations of the source tensor d, as these coefficients are proportional to the projection values of the source tensor onto the eigenspaces of elasticity tensor, namely $(\Sigma^i.\mathbf{d})$. It is therefore important to understand how the values of these projections change with respect to various orientations of the source tensor $\mathbf{d}$.

In this section, for each 10-gridded orientations of the slip and normal vectors around the unit sphere, the values of the projections, namely $(\Sigma^i.\mathbf{d})$, are plotted on the steographic projection net. Fortunately, unlike the entries of the moment tensor, the structure of the moment tensor is not changed with the strike of the fault, in a focal region with a horizontal layering.

The rake and dip angles are therefore sufficient in representing the slip vector and the orientation of the fault. As a point on the net represents a particular fault orientation and slip vector for a fixed strike direction, this characteristics of the TI elasticity tensors with vertical normals enables one to plot the invariants of the moment tensor on a steographic projection net.

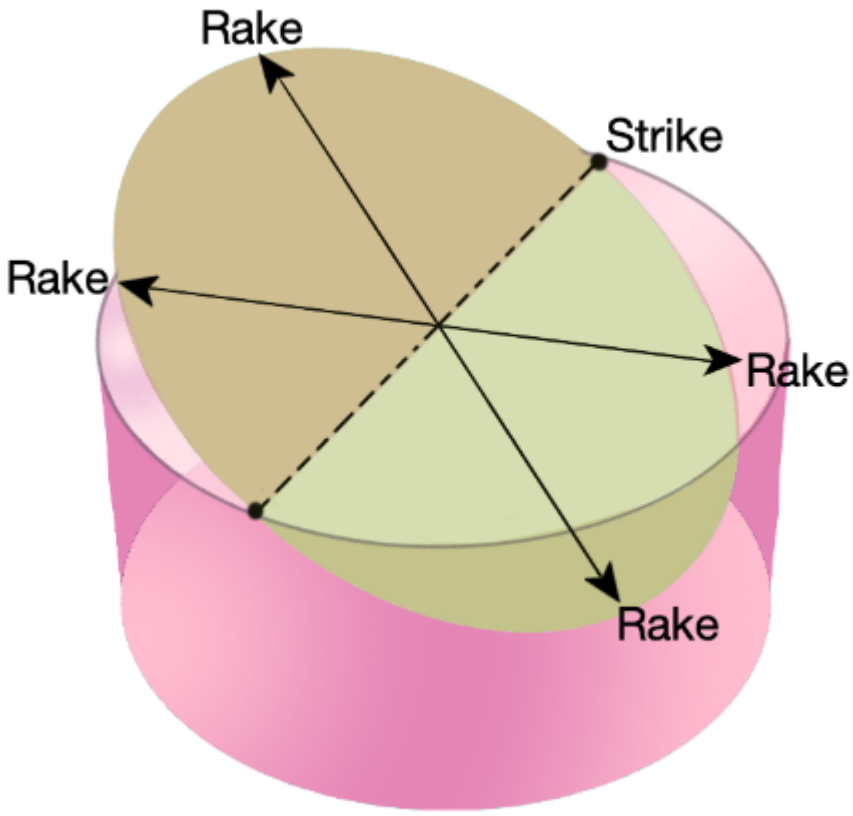

Figure 3.1. Representation of TI medium and fault plane.

where cylinder and circle-shaped plane represent TI medium and dipping fault plane respectively (Figure 3.1). For a TI medium with vertical infinite-fold axis, the structure of the resulting moment tensors are not changed by strike direction.

For different orientations of the fault and slip vector, consider Figure (3.2) for projections values of the source tensor onto the eigenspace $< \Sigma^3, \Sigma^4 >$. $||(\Sigma^3.d)\Sigma^3 + (\Sigma^4.d)\Sigma^4||$ formula is used in calculation of the values of the projections on the two-dimensional eigenspace, written on each point.

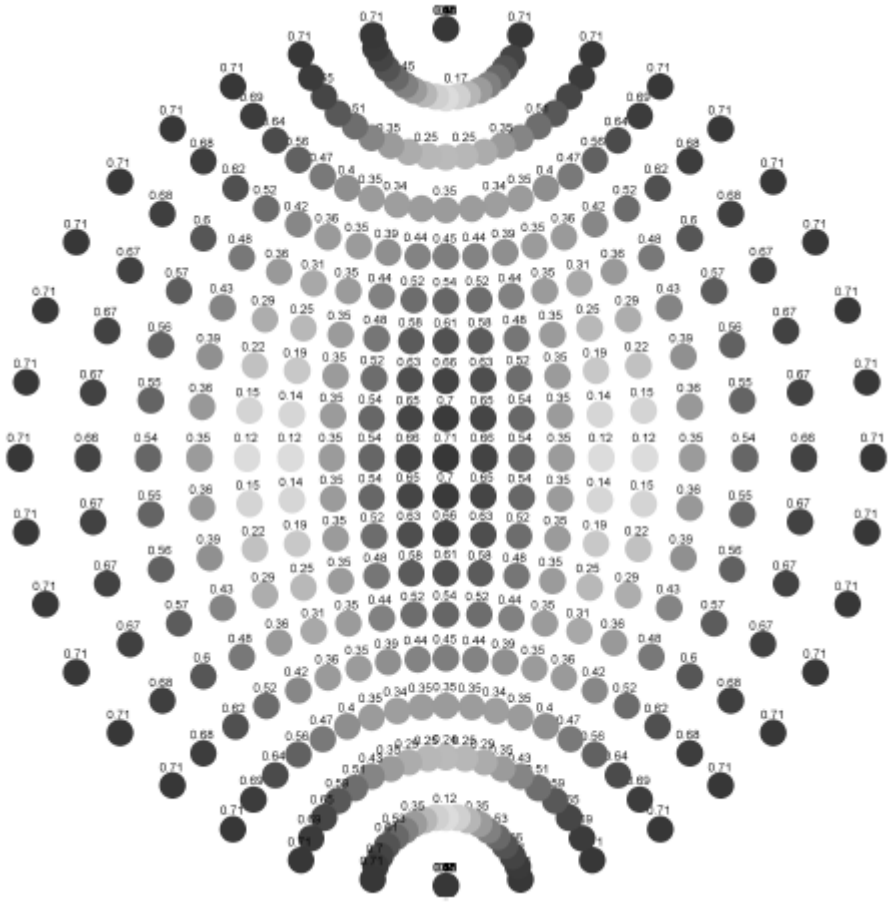

Figure 3.2. The source tensor **d** projections' values onto the eigenspace $< \Sigma^3, \Sigma^4 >$.

In Figure (3.2), each point on the net corresponds to a downward-dipping slip vector on a fault striking North (normal faults). In other words, the net is only plotted with the slip vectors represented by the points on the lower hemisphere. Nevertheless, the projections values are the same for the the slip vectors represented by the points on the upper hemisphere (thrust faults).

For a focal region with a horizontal layering (the xy-plane), this symmetry makes sense as the angle between the slip vector **u** and xy-plane and the angle between the slip vector **-u** and xy-plane are the same. In addition, due to symmetry of TI elasticity tensors with vertical infinite-fold rotation axis (horizontal layerings), there is another significant property of these plots.

Although the space of the source tensors is not completely covered by the source tensors represented by points on the stereographic network, but the values of the projections shown on the graph in Figure (3.2) have been completed. More precisely, some source tensors can only be obtained for faults striking in a different direction from the North, for example $\mathbf{d}$ = (1, 1, 0, 0, 0, 0) can only be obtained when the strike is 45 $^\circ$. Nonetheless, the value of the projection of d onto an eigenspace and the projection of 45-rotated d (hence strike becomes North) onto the eigenspace are the same.

Therefore, in terms of showing all the possible values of the invariants of the moment tensor, such as projections, norms, traces, eigenvalues, the figures are complete.

The source tensor $\mathbf{D}$ is first evaluated using equation (2.18) for the corresponding unit fault normal $\mathbf{n}$ and unit slip vector $\mathbf{u}$, to obtain the values of the projections on the net. Then source vector $\mathbf{d}$ is evaluated using equation (2.21) in Kelvin notation. Note that for unit vectors $\mathbf{n}$ and $\mathbf{u}$, $||\mathbf{d}|| = \frac{1}{\sqrt{2}}$ is equal to 0.71. As a consequence if $\mathbf{d} \in < \Sigma^3, \Sigma^4 >$, naturally, the value of these projection of $\mathbf{d}$ onto the that eigenspace would be 0.71 as well.

Note that the eigenspace $< \Sigma^3, \Sigma^4 >$ is the space which includes any slip directions on xy-plane.In order to make it clear the eigenvector $\Sigma^3 = (0, 0, 0, 1, 0, 0)$ fits to a source whose fault normal is along the z- axis,slip is along the y-axis. Like the Σ^3, if fault normal is along the z-axis and slip is along the x-axis in any source, this corresponds to $\Sigma^4 = (0, 0, 0, 0, 1, 0)$.

Note that the projection values are strongly symmetrical; the first quadrants of the net is repeated in the other three quadrants. As the angles between the slip vectors (u_1, u_2, u_3), (-u_1, u_2, u_3), (u_1, -u_2, u_3), (-u_1, -u_2, u_3) and xy-plane are all identical, where the slip vectors shown above lie in the first, second, third and fourth quadrants, respectively, this is predicted in a focal region with a horizontal layering. Henceforth, only the first quadrant of the stereographic net is going to be plotted due to symmetric property of the plots.

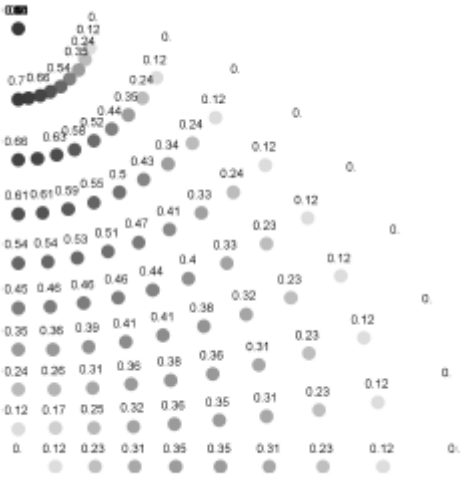

Figure 3.3. The projection of the source tensor **d** onto the eigenspace $< \Sigma^5, \Sigma^6 >$. Only the first quadrant is plotted as the values of the projections in the other three quadrants are symmetrical.

As demonstrated in Figure(3.3) when **u**= $(0, 1, 0)$ and **n** = $(1, 0, 0)$, accordingly **d** = $(0, 0, 0, 0, 0, 1) \in \Sigma^5$ gets the maximum value of the projection onto the eigenspace $< \Sigma^5, \Sigma^6 >$.

It can be noticed that, the projections of source tensors onto the eigenspaces $< \Sigma^3, \Sigma^4 >$ and $< \Sigma^5, \Sigma^6 >$ are almost dual to each other by taking into account Figures (3.2) and (3.3). In other words, along the orientations of source where minimum values are taken by the projections onto $< \Sigma^5, \Sigma^6 >$, the projections onto$< \Sigma^3, \Sigma^4 >$ take maximum values and vice versa. In addition, the white regions (local min) in Figure (3.2), e.g. dip= 50 and rake= 90, becomes black regions (local max) in Figure (3.2). When considering in the next section the norms of moment tensors, this duality relationship between the eigenspaces will be significant.

In Figures (3.5) and (3.4), respectively, the values of the source tensor projections onto the eigenspaces Σ^1 and Σ^2 for different dip and rake values were plotted. These values are important as in the resulting moment tensor they specify almost all of the non-DC components. However, unlike the projections onto $< \Sigma^3, \Sigma^4 >$ and $< \Sigma^5, \Sigma^6 >$, the projections depend the value of γ.

Therefore, each of Figures (3.5) and (3.4) contains two plots showing the projections of different γ values on the eigenspaces, namely, different elasticity tensors listed in Table (3.3) or (3.4).

One of the main characteristics of the Figures (3.2) and (3.3) is that they both attain their maximum and minimum values in the same orientations of the source tensor (the black and white regions are similar). The non-DC components of the resulting moment tensor thus increase along the orientations of the source where both projection values increase (black regions).

It can also be concluded from Figure (3.4) that the values of the projections onto Σ_2 are not responsive to γ; while it is not the case for the projection onto Σ_1.

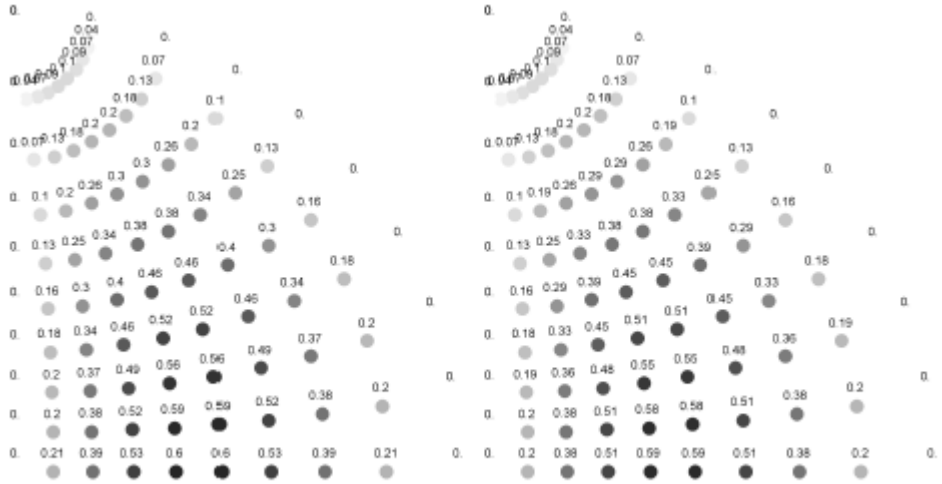

Figure 3.4. The projection of the source tensor $\mathbf{d}$ onto the eigenspace Σ^2 of elasticity tensors of (a) Shale I and (b) Dry Cracks, γ values are 0.77 and 0.55, respectively (Table 3.4). In comparison to the projections onto eigenspaces $< \Sigma^3, \Sigma^4 >$ and $< \Sigma^5, \Sigma^6 >$, the projection onto Σ^2 depends on γ . Observe from the figures, however, that the value of the projection of a shear source onto Σ^2 is not very responsive to γ.

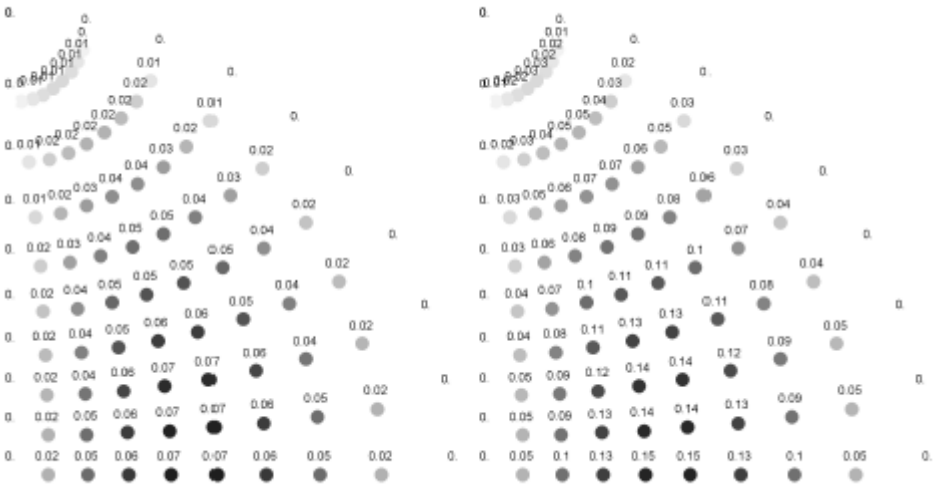

Figure 3.5. The projection of the source tensor **d** onto the eigenspace Σ^1 of elasticity tensors of (a) Shale I and (b) Dry Cracks, where$\gamma = 0.77$ and $\gamma = 0.55$, respectively (Table 3.4). In contrast to the other projections, the projections ontoΣ^1 , i.e. $(\Sigma^1.d)$, have very small values as d is a shear source andΣ^1 is close to the identity matrix.

Table 3.3: Elastic parameters.

Rocks	C_{11}	C_{33}	C_{44}	C_{12}	C_{13}
Dry Cracks	53.51	33.35	14.28	17.79	12.32
Water-Filled Cracks	56.62	56.11	14.28	20.90	20.75
Periodic Thin Layers	32.27	24.84	7.95	11.91	9.51
Sandstone	55.0	46.53	16.26	15.65	20.89
Shale-I	58.81	27.23	13.23	11.73	23.64
Shale-II	34.30	22.70	5.40	13.10	10.70
Gneiss	102.7	71.80	26.90	25.1	25.2
Schist	113.8	88.50	29.9	30.2	23.0
Phyllite	120.2	97.9	32.3	30.3	23.9
Slate	123.3	80.05	21.1	31.3	40.4

Table 3.4: Eigenvalues of materials.

Rocks	λ_1	λ_2	$\lambda_3 = \lambda_4$	$\lambda_5 = \lambda_6$	γ
Dry Cracks	78.09	26.56	28.56	35.72	0.55
Water-Filled Cracks	98.05	35.58	28.56	35.72	0.99
Periodic Thin Layers	51.07	17.95	15.90	20.36	0.72
Sandstone	90.50	26.68	32.52	39.35	0.95
Shale-I	88.72	9.05	26.46	47.08	0.77
Shale-II	54.58	15.52	10.8	21.2	0.62
Gneiss	145.12	54.48	53.8	77.6	0.69
Schist	159.01	73.49	59.8	83.6	0.65
Phyllite	167.03	81.37	64.6	89.9	0.69
Slate	185.65	49.45	42.2	92.0	0.77

3.3. Norm of A Moment Tensor

The norm of moment tensor can be expressed in terms of eigenvectors and eigenvalues of the elasticity tensor of the focal region. This can be done by using eigendecomposition, namely equation (3.5).

Observe that the norm and the eigenvalues of M change as the projection of $\mathbf{d}(\psi, \phi, \xi)$ onto the eigenspaces Σ^i varies for different strike-dip-rake angles. In order to see that the norm of the equation (3.5) should be taken as

$$
\begin{aligned}
||m||^2 &= ||\lambda_1^C(\hat{\mathbf{\Sigma}}^{\mathbf{1}}.\mathbf{d})\hat{\mathbf{\Sigma}}^{\mathbf{1}}||^2 + ||\lambda_2^C(\hat{\mathbf{\Sigma}}^{\mathbf{2}}.\mathbf{d})\hat{\mathbf{\Sigma}}^{\mathbf{2}}||^2 + \qquad (3.7)\\
&\quad ||\lambda_3^C(\hat{\mathbf{\Sigma}}^{\mathbf{3}}.\mathbf{d})\hat{\mathbf{\Sigma}}^{\mathbf{3}}||^2 + ||\lambda_4^C(\hat{\mathbf{\Sigma}}^{\mathbf{4}}.\mathbf{d})\hat{\mathbf{\Sigma}}^{\mathbf{4}}||^2 +\\
&\quad ||\lambda_5^C(\hat{\mathbf{\Sigma}}^{\mathbf{5}}.\mathbf{d})\hat{\mathbf{\Sigma}}^{\mathbf{5}}||^2 + ||\lambda_6^C(\hat{\mathbf{\Sigma}}^{\mathbf{6}}.\mathbf{d})\hat{\mathbf{\Sigma}}^{\mathbf{6}}||^2\\
&\quad \text{Since all } \hat{\Sigma}^i\text{'s are perpendicular to each other,}\\
&= (\lambda_1^C(\hat{\mathbf{\Sigma}}^{\mathbf{1}}.\mathbf{d}))^2 + (\lambda_2^C(\hat{\mathbf{\Sigma}}^{\mathbf{2}}.\mathbf{d}))^2 + (\lambda_3^C(\hat{\mathbf{\Sigma}}^{\mathbf{3}}.\mathbf{d}))^2 + \qquad (3.8)\\
&\quad (\lambda_3^C(\hat{\mathbf{\Sigma}}^{\mathbf{4}}.\mathbf{d}))^2 + (\lambda_5^C(\hat{\mathbf{\Sigma}}^{\mathbf{5}}.\mathbf{d}))^2 + (\lambda_5^C(\hat{\mathbf{\Sigma}}^{\mathbf{6}}.\mathbf{d}))^2\\
&\quad \text{since } ||\hat{\Sigma}^i|| = 1\\
&= (\lambda_1^M)^2 + (\lambda_2^M)^2 + (\lambda_3^M)^2 \qquad (3.9)
\end{aligned}
$$

where the last line demonstrates that the norm square is equal to the to the summation of the squares of the eigenvalues of M, where λ_i^M states the eigenvalues of the moment tensor in term of $i \in \{1, 2, 3\}$.

Due to the fact that the stiffness of the anisotropic focal region is direction-dependent, the norm of the moment tensor depends on slip orientation and normal vectors. Consequently, stiffer direction has greater norm for a unit source tensor.

The norm of a moment tensor can be explicated as seismic moment in anisotropic focal region. In anisotropic focal region seismic moment does mean the norm of a moment tensor. Definition of seismic moment in isotropic focal region can be expressed as

$$M_0 = \mu||u||||n|| = \frac{||m||}{\sqrt{2}} \qquad (3.10)$$

This definition can be interpreted geometrically by the deviatoric eigenspace. In other words, shear source tensor lies only in one of the eigenspaces of isotropic elasticity tensor.

Therefore, the norm of a moment tensor in isotropic focal region can be shown as

$$||m|| = ||\lambda_2^C.d|| = \lambda_2^C||u||||n||\frac{1}{\sqrt{2}} = 2\mu||u||||n||\frac{1}{\sqrt{2}} = \sqrt{2}\mu||u||||n|| \tag{3.11}$$

where $\lambda_2^C = 2.\mu$ and demonstrates the eigenvalue of deviatoric eigenspace, μ is shear modulus and $||d|| = ||u||||n||\frac{1}{\sqrt{2}}$.

Contrary to isotropic focal region,in anisotropic focal region the source tensor **d** does not have to lie in only one of the eigenspaces of anisotropic elasticity tensor.

We can say that norm of the moment tensor hinges on both the eigenvalues of anisotropic elasticity tensor and the projection values of the source tensor onto the eigenspaces, from Eqn (3.7).

The order relations of the eigenvalues of the focal regions elasticity tensors play an important role for the norm of moment tensors. Due to the different orders of eigenvalues, the plot of the norm can be shown in two different forms. Two different forms are shown in Figure (3.6). These forms illustrate either increasing or decreasing directions and also the extremum orientations. The matter is that, Figure (3.6a) shows that,if $\lambda_2 > \lambda_3$ then the orientations where $rake > 50°$ and $40° < dip < 50°$, would become local maximum which is shown as black region.On the other hand, contrary to Figure (3.6a), Figure (3.6b) shows that orientations become local minimum and it is also shown as white region, since $\lambda_3 > \lambda_2$. The boundary region can be observed when dip angel equals to $0°$ and $rake > 40°$. It can also be called as local minimum for Figure (3.6a), and local maximum for Figure (3.6b).

Note that Figure (3.6a) is a combination of Figure (3.3) and Figure (3.4). Likewise Figure (3.6b) is also combinations of Figure (3.2) and Figure (3.3). The order relation of elasticity tensor eigenvalues plays crutial role in understanding the moment tensor structure. In order to consider which terms most dominate the norm, equation (3.15) can be considered.

Figure 3.6. Plot of the norm of the moment tensors for different sources with two different materials which is given in Table (3.4).a) Showing if $\lambda_2 > \lambda_3$ then the orientations where $rake > 50°$. b) Showing when dip angle is $40° < dip < 50°$ the region would become local maximum which is shown as black region. It can be observed that how order relation of eigenvalues affect the form of norm plots.

Both eigenvalues and the projections of source tensor onto the corresponding eigenvalues are used to detect this situation.

According to Table (3.4), λ_1 is the greatest eigenvalue of a TI media.λ_1 would be corresponds to , λ_1^{iso} which is the first eigenvalue of isotropic media. Obviously λ_1 and λ_1^{iso} would be taken into account that they are similar except for one condition. That is γ value can be observed in eigenvectors of TI elasticity tensor. Even if λ_1 is the greatest eigenvalue among the eigenvalues ,its weight on the norm is small. Because the projection has very small value ($\hat{\Sigma}^1.d$) when comparing the other projection values (Figure 3.5).

Generally λ_5 is the second greatest eigenvalue of TI elasticity tensors as a consequence the term $(\lambda_5(\hat{\Sigma}^5.d))^2+(\lambda_5(\hat{\Sigma}^6.d))^2$ dominates the norm. Observing the similarity of the norm plot (Figure 3.6a) and the projection onto the eigenspace $< \Sigma^5, \Sigma^6 >$ may be helpful to infere this fact. In Figure 3.6a, the black region, where $rake > 40^\circ$ and $40^\circ < dip < 50^\circ$, is more highlighted due to the term $(\lambda_2(\hat{\Sigma}^2.d))^2$ (Eqn 3.7) can be considered as an one and only difference and it dominates those orientation (Figure 3.4). Besides that in Figure (3.6b) same region which is illustrated as white becomes local minimum due to the term $(\lambda_3(\hat{\Sigma}^3.d + \hat{\Sigma}^4.d))^2$ sharply decreases (Figure 3.2).

Therefore, eigenvalues of elasticity tensors have an important role in terms of the variation of the norm of moment tensor for different slip orientations and normal vectors if λ_{min} and λ_{max} are the minimum and maximum eigenvalues of TI elasticity tensor, but λ_1 the variation of norm can be considered as with ratio $\frac{\lambda_{min}}{\lambda_{max}}$.

For example, the eigenvalues of slate are given in Table 3.4. It has the ratio $\frac{\lambda_{min}}{\lambda_{max}} = \frac{42.2}{92} = 0.4587$. Then when we look at the ratio of maximum and minimum values of the norm for different orientations (Figure 3.7) it will be $\frac{29.84}{65.05} = 0.4587$.

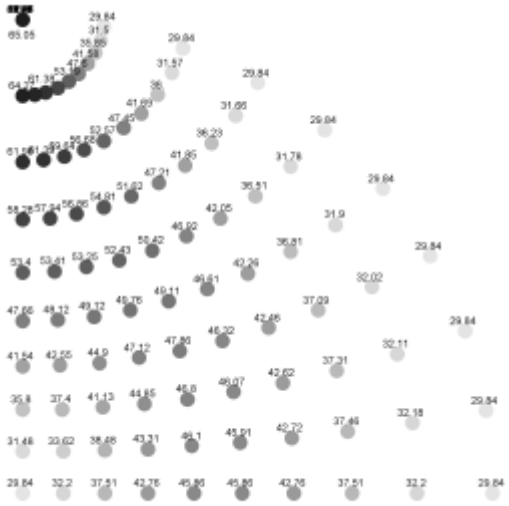

Figure 3.7. Plot of the norm of the moment tensors of source with the eigenvalues of Slate. (3.4).

As we have mentioned above,the order relation of eigenvalues affect the form of norm plots. Therefore in Figure (3.7) order relation of eigenvalues of slate is stated as $\lambda_3 < \lambda_2 < \lambda_5$ (Table 3.4). λ_1 is neglected due to its weight on the norm is very small. As a result, the eigenvalues of elasticity tensor of the focal region dominate the variation of the norm of the moment tensor.

3.4. Isotropic Components of Moment Tensors

The percentage of the isotropic-component of a moment tensor hinges on the slip and normal vectors. Unlike isotropic focal region, in anisotropic region, the shear source may lead to isotropic component.

Note that the word "isotropic" has used in two different ways before. The first "isotropic" means the isotropy class of the four-rank elasticity tensors. Then the second one will be used for expressing the isotropic-component of moment tensor.

In Equation (3.5) , two terms specifies the amount of isotropic component of a moment tensor which includes the eigenspaces Σ^1 and Σ^2. Since the other eigenspaces have no trace, the rest of the terms does not contribute to isotropic component.

In Table (3.2), the eigenspaces Σ^1 and Σ^2 have γ parameter where γ determines the amount of isotropic-component of moment tensor. In order to clarify that, if γ equals to 1 due to $\Sigma^1.d = 0$ and eigenspaces Σ^2 becomes traceless then the shear source doesn't lead to isotropic-component. Determining the amount of isotropic component can be done by understanding the deviation of gamma. If we want to rephrase this determining the amount of isotropic component can be done by understanding the deviation of γ. The isotropic component of moment tensor can be derived from equation (3.5) as

$$\begin{aligned}\mathbf{m}^{iso} = \lambda_1^C(\Sigma^1.d)(\frac{2+\gamma}{3}, \frac{2+\gamma}{3}, \frac{2+\gamma}{3}, 0, 0, 0)\frac{1}{\sqrt{2+\gamma^2}} \\ +\lambda_2^C(\Sigma^2.d)(\frac{2\gamma-2}{3}, \frac{2\gamma-2}{3}, \frac{2\gamma-2}{3}, 0, 0, 0)\frac{1}{\sqrt{2\gamma^2+4}}\end{aligned} \tag{3.12}$$

where the vectors are isotopic components of Σ^1 and Σ^2.

Vavrycuk has used the formula which is mentioned below, in order to estimate the isotropic percentage of given moment tensor Eqn (3.13) [29].

$$ISO = \frac{1}{3}\frac{Trace(\mathbf{M})}{|M_{|MAX|}|}.100 \tag{3.13}$$

Equation (3.13) can be revised as belowed formula. In Equation (3.12) ratio of the eigenvalues of isotopic component and the moment tensor are used to evaluate of isotopic percentage for given moment tensor.

$$\begin{aligned}ISO\% = & \frac{\lambda^{iso}}{\lambda_{max}}.100 \\ = & \frac{1}{3}\frac{Tr(\mathbf{m})}{\lambda_{max}}\end{aligned} \tag{3.14}$$

where λ^{iso} is eigenvalue of the isotropic component of $\mathbf{m}^{iso}$ which is shown in Eqn (3.12). Another term $Tr(\mathbf{m})$ is trace of $\mathbf{m}$. In addition to this, due to the fact that norm of the isotopic component and the moment tensor are related by the formula, they both can be used for calculating the isotropic percentage.

$$||\mathbf{m}||^2 = ||\mathbf{m}^{iso}||^2 + ||\mathbf{m}^{dev}||^2 \tag{3.15}$$

where the term $\mathbf{m}^{dev}$ is deviatoric component of the moment tensor. The above formula is valid due to the fact that the both isotropic spaces and deviatoric spaces are orthogonal subvector spaces of second rank tensors. After that the percentage can be gained as follows

$$\begin{aligned} ISO\% &= \frac{||\mathbf{m}^{iso}||^2}{||\mathbf{m}||^{\mathbf{2}}}.100 && (3.16)\\ &= \frac{||\frac{TR(\mathbf{m}}{3}(1,1,1,0,0,0)||^2}{||\mathbf{m}||^2}.100 && (3.17)\\ &= (\frac{Tr(\mathbf{m}}{\sqrt{3}||\mathbf{m}||_F})^2.100 && (3.18) \end{aligned}$$

The CLVD and DC component share remaining percentage.

Following figures are derived from the formulas (3.14) and (3.16). For different orientations of the source, the variation of the isotropic percentage is showed in Figure (3.9).

Figure (3.8a) shows the distribution of the isotropic percentage of the moment tensor which has different source orientations. This distribution is evaluated using the formula (3.16). But the Figure (3.8b) is evaluated by using the formula (3.14).Both two figures are prepared for ($\gamma = 0.55$)

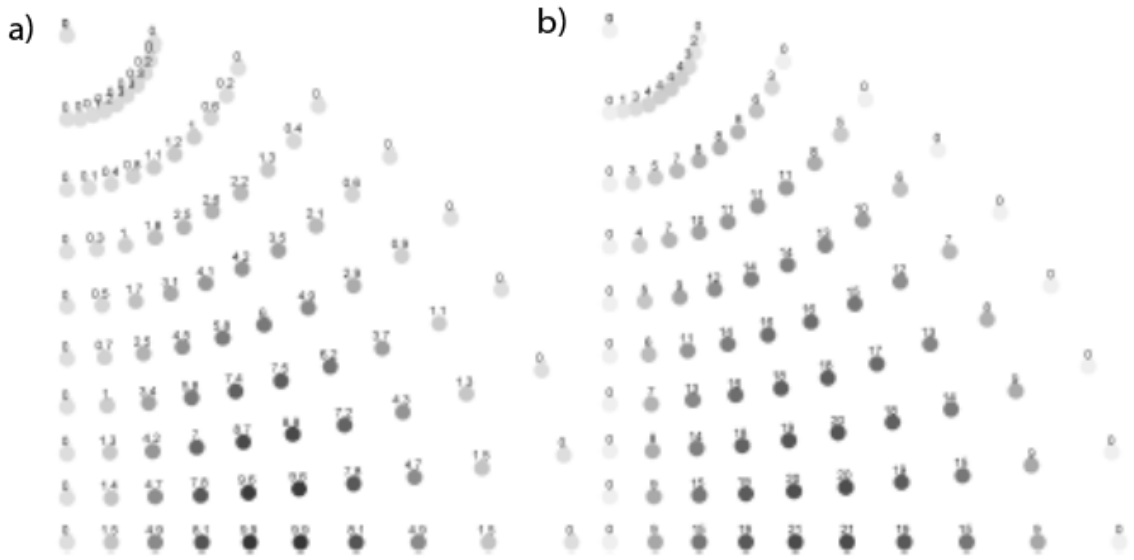

Figure 3.8. Distribution of the isotropic percentages of the moment tensor.a)the distribution of the isotropic percentage of the moment tensor which has different source orientations using the formula (3.16).b)the distribution of the isotropic percentage of the moment tensor using the formula (3.14).

One of the significant differences between the formulas is that Equation(3.14) is used in order to find isotopic percentage. After determining the isotopic percentage, for formula (3.14) the remaining percentages for deviatoric parts also must be calculated. The formulas about remaining parts has shown as follows [29]

$$CLVD\% = 2\epsilon(100\% - |ISO|) \tag{3.19}$$

$$DC\% = 100\% - |ISO| - |CLVD| \tag{3.20}$$

The deviatoric parts which are CLVD and DC components can be obtained using the formulas (3.19,3.20)as follows

$$CLVD\% = 2\epsilon(100\% - ISO\%) \tag{3.21}$$

$$DC\% = (100\% - ISO\% - CLVD\%) \tag{3.22}$$

where ϵ implies the ratio of minimum eigenvalue and maximum eigenvalue of the deviatoric part. Considering the above equations, the isotropic percentage is subtracted in order to ensure that the sum of the components is 100%. That is to say, these formulas do not take advantage of the orthogonality of isotropic and deviatoric subspaces. Nevertheless, CLVD space and DC tensors are not vector spaces, and this is also the reason why it is not unique in moment tensor decomposition.

Figures (3.8 and 3.9) imply the variety of the isotropic percentages for different source orientations.

It is observed that the isotropic percentages decrease as the γ values approach to the unity due to the traces of moment tensors get closer to zero.

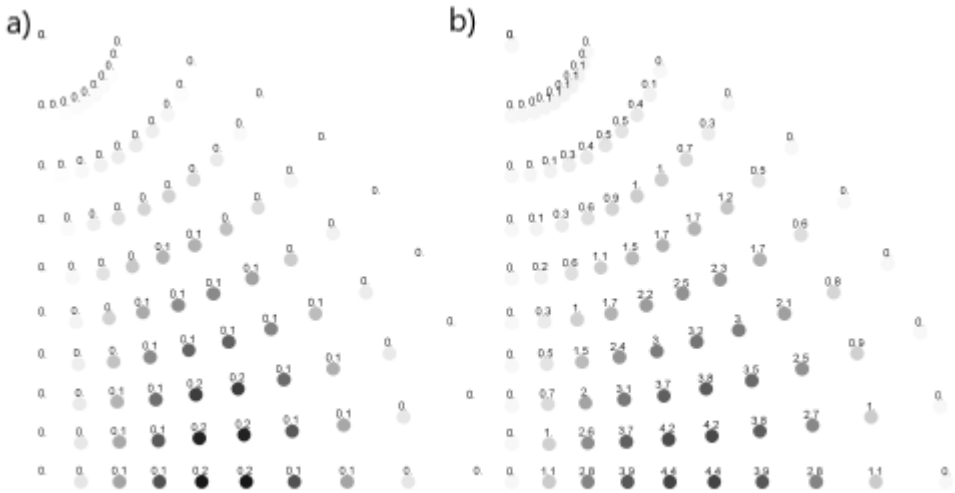

Figure 3.9. The distribution of the isotropic percentages for different sources.a) Prepared for sandstone($\gamma = 0.95$) focal region with the elasticity tensor which indicated in Table(3.4).b) Prepared for slate ($\gamma = 0.77$)

Figure (3.9) shows the distribution of the isotropic percentage of the moment tensor which has different source orientations. This distribution is evaluated using the formula Figure (3.16). Figure(3.9a) is prepared for sandstone($\gamma = 0.95$) focal region with the elasticity tensor which indicated in Table(3.4). On the other hand Figure (3.9b) is prepared for slate ($\gamma = 0.77$).

3.5. Eigenvalues of Moment Tensor

The eigenvalues of the moment tensor determines the mechanism of seismic source. In anisotropic focal regions, unlike isotropy, the eigenvalues of moment tensor varies for every orientation of the slip and normal vectors. Consequently,these orientations affects the radiation pattern of the seismic source significantly.

The following Figure (3.10) illustrates the eigenvalues of moment tensors for different anisotropic focal regions on a fundamental lune [25]. With regard to Figure (3.10) isotropic component amount increases as γ values decrease.

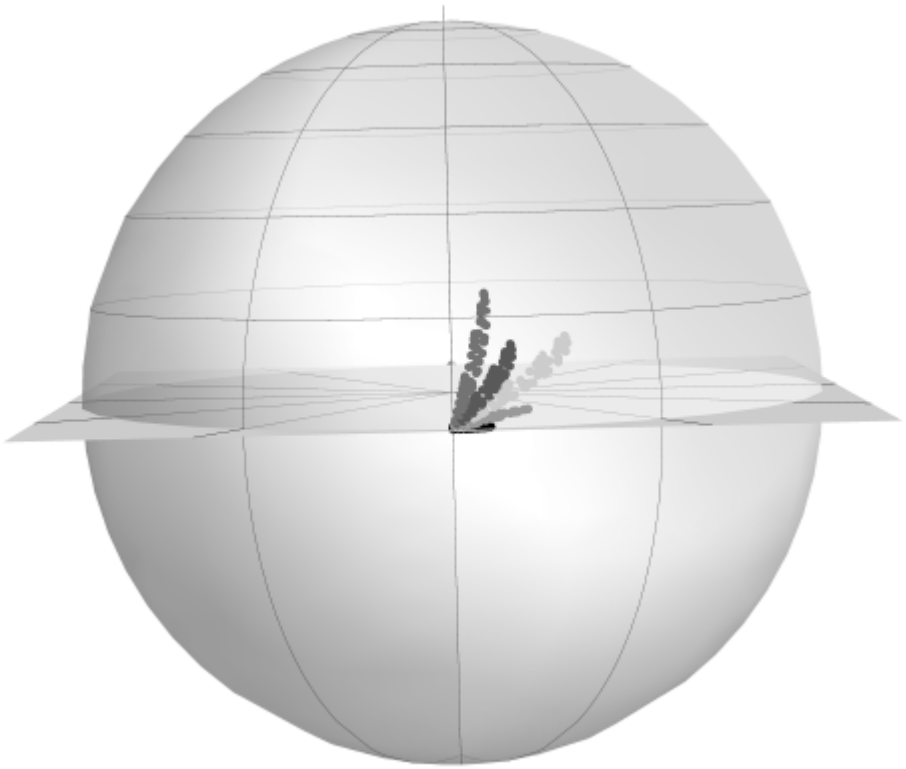

Figure 3.10. Basic lune is showing the eigenvalues of moment tensors of seismic sources occurring in different anisotropic focal regions.

In order to plot the eigenvalues on a unit sphere, the eigenvalues are performed by unit vector $(\lambda_1, \lambda_2, \lambda_3)$ with $\lambda_1 \geq \lambda_2 \geq \lambda_3$. The deviatoric moment tensors imply the equatorial curve and pure explosion i.e. isotropic moment tensor performed on north-pole. The equatorial curves are cut by the vertical curves from left to right which are pure CLVD(2,-1,-1), pure DC (1,0,-1), pure CVLD(1,1,-2). In Table (3.4), elasticity tensor of Water-filled Cracks is given as (0.99) and the black dots which is very near to the equatorial curve that means deviatoric moment tensors. And implies the eigenvalues of moment tensor eventuated in that focal region. From down to up ,the other moment tensors are performed for some focal regions with different elasticity tensors which are given in Table (3.4) such as Sandstone(0.95),Slate(0.77),Gneiss(0.69) and Dry-Cracks(0.55). Consequently, as much as the γ values decrease, the amount of isotropic percentage of moment tensors would be increased oppositely.

3.6. Deviation of Eigenvectors

The testatum formulas are used to determine the orientations of source from the eigenvectors of the moment tensor in isotropic focal regions generally.

$$[\hat{u}] = \frac{1}{\sqrt{2}}(\hat{e_1} + \hat{e_2}) \tag{3.23}$$

$$[\hat{n}] = \frac{1}{\sqrt{2}}(\hat{e_1} - \hat{e_2}) \tag{3.24}$$

where $\hat{u}$ corresponds to unit slip vector and similary $\hat{n}$ is the unit normal vectors. Both $\hat{u}$ and $\hat{n}$ are the unit eigenvectors. Those eigenvectors correspond to moment tensors non-zero eigenvectors. In this case, it is supposed that source region is shear. In other words for this case we can presume $\hat{\mathbf{u}}.\hat{\mathbf{n}} = 0$

In an anisotropic focal region eqn (3.23) and eqn (3.24) are not valid. We expect that, eigenvectors of moment tensor should be aligned along the $\hat{u}$ and $\hat{n}$'s bisectors. But in anisotropic focal region this is not the case . For this reason, we want to know that how much anisotropic elasticity tensor rotates the eigenvectors of the source tensor. Then, deriving the source orientations from the eigenvectors of moment tensor process, the amount of error can be found this way.

The strength at anisotropy can be related with the deviations of the eigenvectors of the moment tensor. The strength of anisotropy is shown in (Table 3.5). In other words, the strength of anisotropy means the distance of elasticity tensors to isotropic symmetry class.

Table 3.5: The strength of anisotropy.

Rocks	λ_1^{iso}	λ_2^{iso}	λ_1^{TI}	$\frac{\lambda_2^{TI}+2\lambda_3^{TI}+2\lambda_5^{TI}}{5}$	Deviation of eigenvalues from C^{ISO}
Dry Cracks	75.0767	31.6267	78.0857	31.0249	13.1523
Water-Filled Cracks	98.05	32.828	98.0515	32.8277	4.268
Periodic Thin Layers	50.4133	18.2253	51.0747	18.0931	4.8284
Sandstone	90.4633	34.0933	90.4997	34.0861	7.6786
Shale-I	87.6233	31.4453	88.7176	31.2265	24.7698
Shale-II	53.4333	16.1333	54.5821	15.9036	6.8717
Gneiss	142.733	63.9333	145.122	63.456	18.4763
Schist	156.167	72.6267	159.006	72.0588	17.2857
Phyllite	164.833	78.5333	167.027	78.0947	16.2781
Slate	183.767	63.9467	185.646	63.5709	28.0533

In Table (3.5), the first two columns indicates that the given TI tensors eigenvalues of the closest isotropic elasticity tensor. Herein, C^{iso} is the closest isotropic tensor. When taking the orthogonal projection of the C^{TI} onto the elasticity tensors isotropic linear subspace, C^{iso} is found. In Table (3.5), last column means the distance.

This distance can be found as norm of difference of C^{TI} and C^{iso}. The third and fourth columns indicate the eigenvalues of C^{iso}. It may also be approximated using Eqns (2.34) and (2.35).

Figures (3.11,3.12,3.13 and 3.14) illustrate the deviation angles of the eigenvectors for different source orientations. In those figures, it is obvious that deviation angles decrease as the elasticity tensors get closer to isotropy.

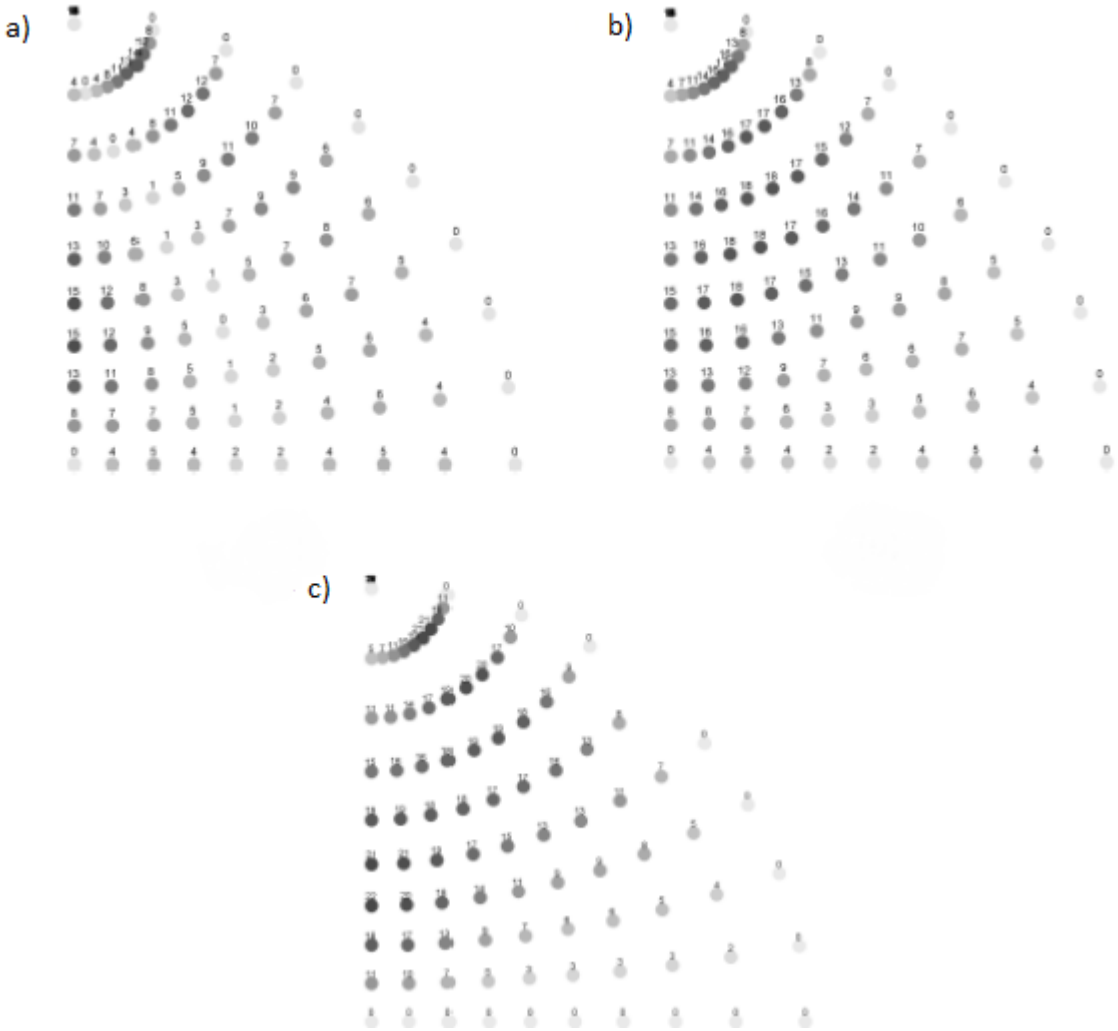

Figure 3.11. Deviations of eigenvectors are shown and elasticity tensor of Slate is used. The eigenvectors which is shown above account for a) positive b) negative c) near to zero eigenvalues, respectively.

In Figure (3.11) elasticity tensor of the Slate is used which is given in Table (3.5). The distance to isotropy of Slate is 28.05. The eigenvectors which is shown above account for a) positive b) negative c) near to zero eigenvalues, respectively. With these plots, how much does the elasticity tensor rotate the source tensors eigenvector can be found by performed $m_{ij} = C_{ijkl}.d_{kl}$. To remind, in isotropic focal regions source tensors eigenvectors and moment tensors eigenvectors are parallel.

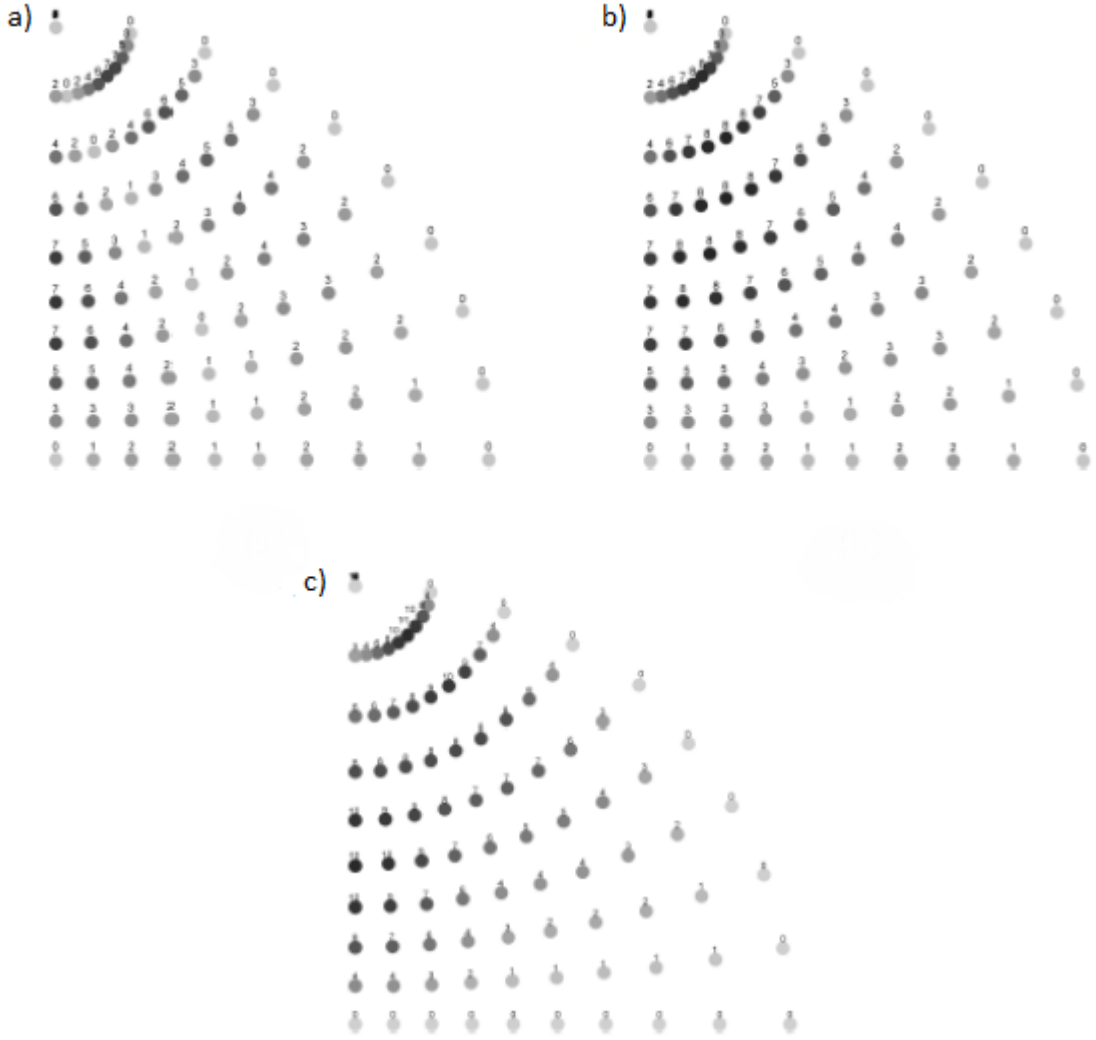

Figure 3.12. Deviations of eigenvectors are shown and elasticity tensor of Gneiss is used. Distance is given as 18.476 in Table (3.5). The eigenvectors which is shown above account for a) positive b) negative c) near to zero eigenvalues, respectively.

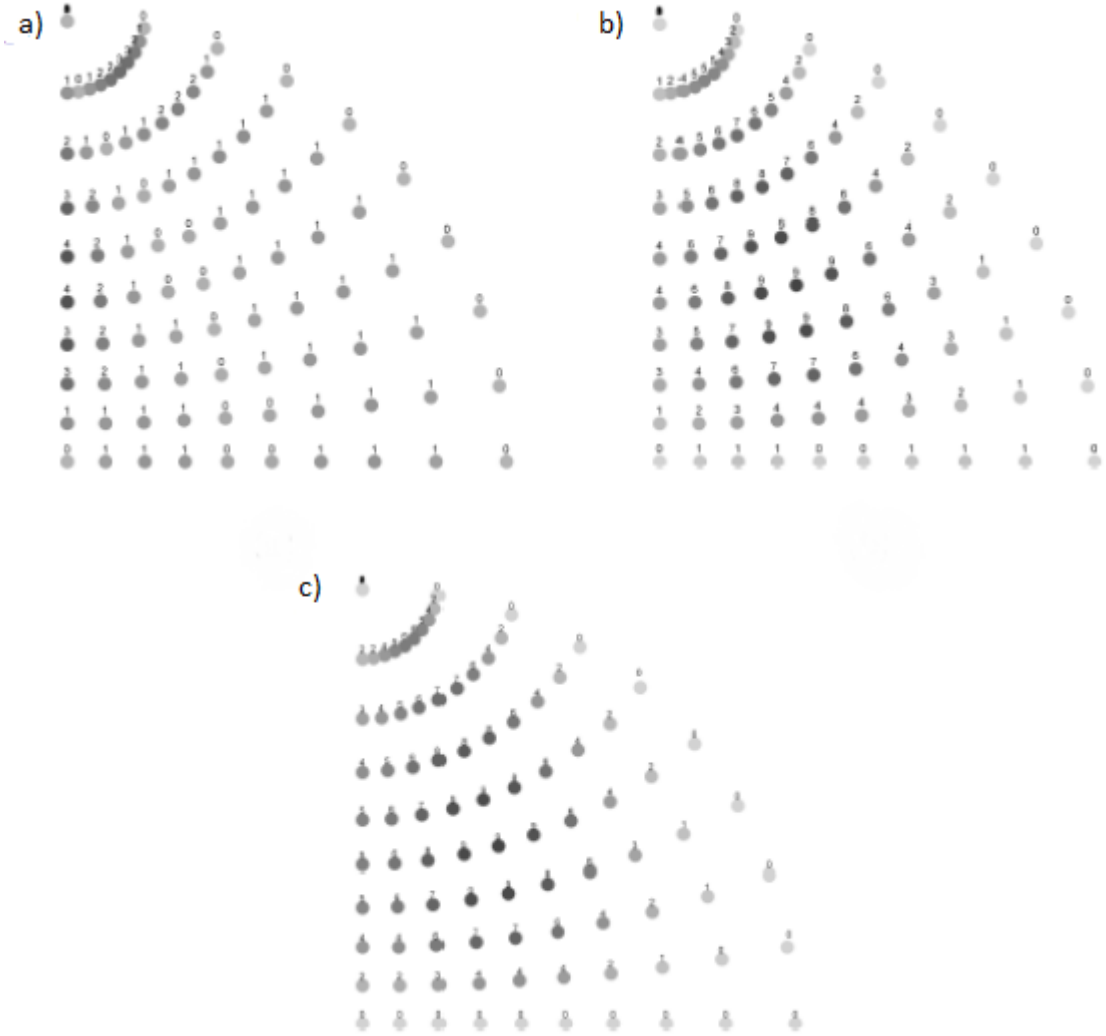

Figure 3.13. Deviations of eigenvectors are shown and elasticity tensor of Sandstone is used. Distance of Sandstone is 7.68 (Table 3.5). The eigenvectors which is shown above account for a) positive b) negative c) near to zero eigenvalues, respectively.

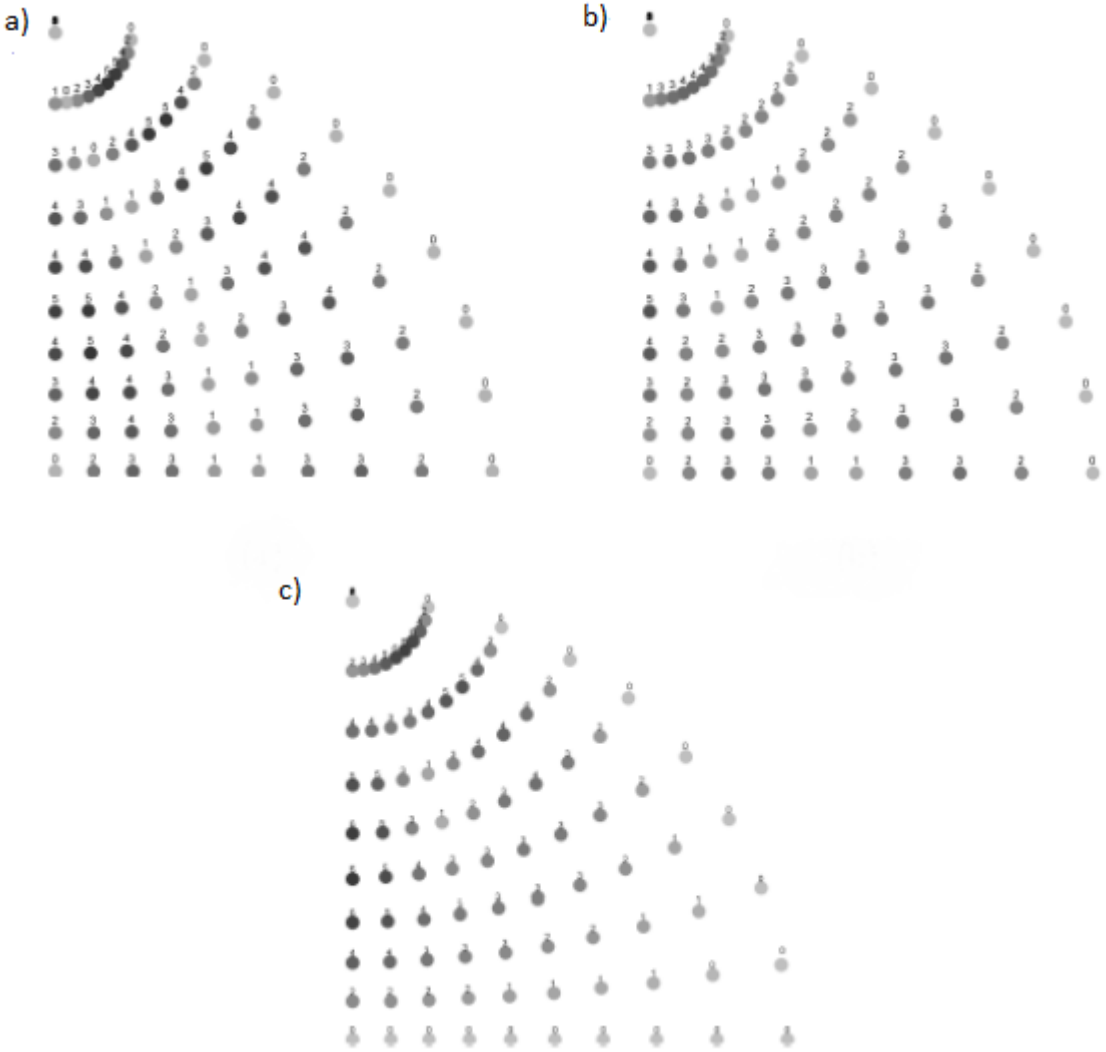

Figure 3.14. Deviations of eigenvectors are shown and elasticity tensor of Water-filled cracked is used. Distance of water-filled cracks is 4.268 (Table 3.5). The eigenvectors which is shown above account for a) positive b) negative c) near to zero eigenvalues, respectively.

4. CONCLUSIONS

Conclusion can be summarized as follows;

i. The structure of the moment tensor of shear sources occuring in vertical TI focal region depends on two angles;the angle between the normal vector of fault and the infinite-fold rotation axis of TI elasticity tensor, and the angle between the slip and the symmetry plane of the TI elasticity tensor.

ii. The structure of the moment tensor does not changed with the strike of the fault, in a focal region with a horizontal layering.

iii. The stiffness of the anisotropic focal region is direction-dependent hence the norm of the moment tensor depends on slip orientation and normal vectors. Consequently, stiffer direction has greater norm for a unit source tensor.

iv. Norm of the moment tensor hinges on both the eigenvalues of anisotropic elasticity tensor or projection values of the source tensor onto the eigenspaces.

v. Both eigenspaces and the projections of source tensor onto the corresponding eigenvalues are used to detect which terms dominate the norm most.

vi. The order relation of eiagenvalues determines the extremum orientations of the norm.

vii. The ratio of maximum and minimum norm is equal to the variation of the maximum and minimum eigenvalues excluding λ_1.

viii. The value of "γ" determines the amount of isotropic-component of moment tensor. A shear source in TI focal region does not lead to isotropic-component whenever γ=1.

ix. Isotropic component increases as γ values decrease.

REFERENCES

1. Keiiti Aki and Paul G Richards. *Quantitative seismology*. 2002.

2. Vladislav Babuska and Michel Cara. *Seismic anisotropy in the Earth*, volume 10. Springer Science & Business Media, 1991.

3. A Ben-Menahem and AG Sena. The elastodynamic green's tensor in an anisotropic half-space. *Geophysical Journal International*, 102(2):421–443, 1990.

4. Ari Ben-Menahem, Richard L Gibson Jr, and Arcangelo G Sena. Green's tensor and radiation patterns of point sources in general anisotropic inhomogeneous elastic media. *Geophysical journal international*, 107(2):297–308, 1991.

5. Ari Ben-Menahem and Arcangelo G Sena. Seismic source theory in stratified anisotropic media. *Journal of Geophysical Research: Solid Earth*, 95(B10):15395–15427, 1990.

6. Andrej Bóna, Ioan Bucataru, and Michael A Slawinski. Coordinate-free characterization of the symmetry classes of elasticity tensors. *Journal of Elasticity*, 87(2-3):109–132, 2007.

7. R Burridge. The singularity on the plane lids of the wave surface of elastic media with cubic symmetry. *The Quarterly Journal of Mechanics and Applied Mathematics*, 20(1):41–56, 1967.

8. R Burridge and L Knopoff. Body force equivalents for seismic dislocations. *Bulletin of the Seismological Society of America*, 54(6A):1875–1888, 1964.

9. Vlastislav Cerveny. *Seismic ray theory*. Cambridge university press, 2005.

10. Cliff Frohlich. Earthquakes with nondouble-couple mechanisms. *Science*, 264(5160):804–809, 1994.

11. Dirk Gajewski. Radiation from point sources in general anisotropic media. *Geophysical Journal International*, 113(2):299–317, 1993.

12. K Helbig. Foundations of anisotropy for exploration seismics, 486 pp. *NY: Elsevier*, 1994.

13. Bruce R Julian, Angus D Miller, and GR Foulger. Non-double-couple earthquakes 1. theory. *Reviews of Geophysics*, 36(4):525–549, 1998.

14. Hitoshi Kawakatsu. Enigma of earthquakes at ridge-transform-fault plate boundaries distribution of non-double couple parameter of harvard cmt solutions. *Geophysical Research Letters*, 18(6):1103–1106, 1991.

15. Ichiro Kawasaki and Toshiro Tanimoto. Radiation patterns of body waves due to the seismic dislocation occurring in an anisotropic source medium. *Bulletin of the Seismological Society of America*, 71(1):37–50, 1981.

16. Leon Knopoff and Michael John Randall. The compensated linear-vector dipole: A possible mechanism for deep earthquakes. *Journal of Geophysical Research*, 75(26):4957–4963, 1970.

17. Angus D Miller, GR Foulger, and Bruce R Julian. Non-double-couple earthquakes 2. observations. *Reviews of Geophysics*, 36(4):551–568, 1998.

18. MJP Musgrave. *Crystal acoustics*. Acoustical Society of America New York, 2003.

19. Ivan Pšenčík. Green's functions for inhomogeneous weakly anisotropic media. *Geophysical Journal International*, 135(1):279–288, 1998.

20. Wolfgang Rabbel and Walter D Mooney. Seismic anisotropy of the crystalline crust: what does it tell us? *Terra Nova*, 8(1):16–21, 1996.

21. Dirk Rössler, G Rümpker, and Frank Krüger. Ambiguous moment tensors and radiation patterns in anisotropic media with applications to the modeling of earth-

quake mechanisms in w-bohemia. *Studia Geophysica et Geodaetica*, 48(1):233–250, 2004.

22. Vladimír Rudajev and Jan Šílenỳ. Seismic events with non-shear component: Ii. rock bursts with implosive source component. *Pure and Applied Geophysics*, 123(1):17–25, 1985.

23. MK Savage. Seismic anisotropy and mantle deformation: what have we learned from shear wave splitting? *Reviews of Geophysics*, 37(1):65–106, 1999.

24. Jan Šílenỳ and Alexander Milev. Source mechanism of mining induced seismic eventsresolution of double couple and non double couple models. *Tectonophysics*, 456(1-2):3–15, 2008.

25. Walter Tape and Carl Tape. A geometric setting for moment tensors. *Geophysical Journal International*, 190(1):476–498, 2012.

26. Václav Vavryčuk. Elastodynamic and elastostatic green tensors for homogeneous weak transversely isotropic media. *Geophysical Journal International*, 130(3):786–800, 1997.

27. Václav Vavryčuk. Non-double-couple earthquakes of 1997 january in west bohemia, czech republic: evidence of tensile faulting. *Geophysical Journal International*, 149(2):364–373, 2002.

28. Václav Vavryčuk. Inversion for anisotropy from non-double-couple components of moment tensors. *Journal of Geophysical Research: Solid Earth*, 109(B7), 2004.

29. Václav Vavryčuk. Focal mechanisms in anisotropic media. *Geophysical Journal International*, 161(2):334–346, 2005.

30. Václav Vavryčuk. Moment tensor decompositions revisited. *Journal of Seismology*, 19(1):231–252, 2015.

31. Václav Vavryćuk. Moment tensors: Decomposition and visualization. 2015.